Bioorganic Chemistry 112 (2021) 104919

Contents lists available at ScienceDirect

Bioorganic Chemistry

journal homepage: www.elsevier.com/locate/bioorg

Concise synthesis and biological evaluation of 2-Aryl-3-Anilinobenzo[*b*]thiophene derivatives as potent apoptosis-inducing agents

Romeo Romagnoli [a,*], Delia Preti [a], Ernest Hamel [b], Roberta Bortolozzi [c], Giampietro Viola [c,d], Andrea Brancale [e], Salvatore Ferla [f], Giampaolo Morciano [g], Paolo Pinton [g]

[a] *Dipartimento di Scienze Chimiche, Farmaceutiche ed Agrarie, Via Luigi Borsari 46, Università degli Studi di Ferrara, 44121 Ferrara, Italy*
[b] *Molecular Pharmacology Branch, Developmental Therapeutics Program, Division of Cancer Treatment and Diagnosis, Frederick National Laboratory for Cancer Research, National Cancer Institute, National Institutes of Health, Frederick, MD 21702, USA*
[c] *Dipartimento di Salute della Donna e del Bambino, Laboratorio di Oncoematologia, Università di Padova, 35131 Padova, Italy*
[d] *Istituto di Ricerca Pediatrica (IRP), Corso Stati Uniti 4, 35128 Padova, Italy*
[e] *School of Pharmacy and Pharmaceutical Sciences, Cardiff University, King Edward VII Avenue, Cardiff CF10 3NB, UK*
[f] *Swansea University Medical School, Institute of Life Sciences 2, Swansea University, Swansea SA2 8PP, UK*
[g] *Department of Medical Sciences, Laboratory for Technologies of Advanced Therapies (LTTA), University of Ferrara, 44121 Ferrara, Italy*

ARTICLE INFO

Keywords:
Microtubules
Benzo[*b*]thiophene
Apoptosis
Alteration of mitochondrial function

ABSTRACT

Many clinically used agents active in cancer chemotherapy exert their activity through the induction of cell death (apoptosis) by targeting microtubules, altering protein function or inhibiting DNA synthesis. The benzo[*b*]thiophene scaffold holds a pivotal place as a pharmacophore for the development of anticancer agents, and, in addition, this scaffold has many pharmacological activities. We have developed a flexible method for the construction of a new series of 2-aryl-3-(3,4,5-trimethoxyanilino)-6-methoxybenzo[*b*]thiophenes as potent antiproliferative agents, giving access to a wide range of substitution patterns at the 2-position of the 6-methoxybenzo[*b*]thiophene common intermediate. In the present study, all the synthesized compounds retained the 3-(3,4,5-trimethoxyanilino)-6-methoxybenzo[*b*]thiophene moiety, and the structure–activity relationship was examined by modification of the aryl group at its 2-position with electron-withdrawing (F) or electron-releasing (alkyl and alkoxy) groups. We found that small substituents, such as fluorine or methyl, could be placed in the *para*-position of the 2-phenyl ring, and these modifications only slightly reduced antiproliferative activity relative to the unsubstituted 2-phenyl analogue. Compounds **3a** and **3b**, bearing the phenyl and *para*-fluorophenyl at the 2-position of the 6-methoxybenzo[*b*]thiophene nucleus, respectively, exhibited the greatest antiproliferative activity among the tested compounds. The treatment of both Caco2 (not metastatic) and HCT-116 (metastatic) colon carcinoma cells with **3a** or **3b** triggered a significant induction of apoptosis as demonstrated by the increased expression of cleaved-poly(ADP-ribose) polymerase (PARP), receptor-interacting protein (RIP) and caspase-3 proteins. The same effect was not observed with non-transformed colon 841 CoN cells. A potential additional effect during mitosis for **3a** in metastatic cells and for **3b** in non-metastatic cells was also observed.

1. Introduction

Among different strategies used for cancer chemotherapy, the identification of compounds that induce apoptosis (programmed cell death) in cancer cells is recognized as an important approach for the discovery of new anti-cancer agents [1–3]. Molecules that interfere with the microtubule system usually cause a major increase in apoptosis in cancer cells sensitive to these agents [4–7].

Microtubules are cylindrical structures of great length formed by the polymerization of αβ-tubulin heterodimers [8], and these structures are dynamic components of the cytoskeleton of eukaryotic cells [9]. Functions of microtubules include the formation of the mitotic spindle, required for separation of duplicated chromosomes before cell division, determination and maintenance of cell shape, regulation of motility and signaling, secretion and organelle transport inside the cell [10]. The microtubule spindle of dividing cells is especially remarkable in that it

* Corresponding author.
E-mail address: rmr@unife.it (R. Romagnoli).

https://doi.org/10.1016/j.bioorg.2021.104919
Received 10 March 2021; Received in revised form 12 April 2021; Accepted 14 April 2021
Available online 20 April 2021

forms and disappears rapidly during the 10–15 min of the M phase of the cell cycle. The biological importance of microtubules makes them an interesting target for the development of anticancer drugs [11–14].

Numerous chemically diverse substances disrupt the formation of the mitotic spindle, and these can be divided into microtubule stabilizing and destabilizing agents [15,16]. While both groups cause mitotic arrest and subsequent apoptosis, the destabilizing agents specifically inhibit tubulin assembly into microtubules and can cause the disassembly of pre-existing microtubules [17,18].

Among the natural microtubule depolymerizing agents, combretastatin A-4 (CA-4, **1a**, Fig. 1) is one of the more studied antimitotic agents [19]. CA-4, isolated from the bark of the South African tree *Combretum caffrum,* strongly and reversibly inhibits the polymerization of tubulin through a strong interaction with the colchicine site of tubulin [20].

Despite the synthesis of many tubulin inhibitors, there remains a need to identify novel small molecules that target microtubules [21–23]. Limited examples of tubulin polymerization inhibitors (TPIs) based on the chemical structure of the benzo[*b*]thiophene molecular structure have been reported. Among them, Pinney and co-workers reported several TPIs with general structure **2** characterized by the presence of the 2-aryl-3-substituted-6-methoxybenzo[*b*]thiophene structural motif as its core structure [24].

Compound **2a**, based on the 2-(4-methoxyphenyl)-3-(3,4,5-trimethoxybenzoyl)-benzo[*b*]thiophene ring system, has unusual inhibitory effects on tubulin polymerization, with inhibition of the rate of assembly up to about 3–4 μM and a partial effect on tubulin polymerization at a concentration of 40 μM. At a concentration of 50 μM, this derivative shows a modest inhibition (28%) of the binding of [^{3}H]colchicine to tubulin. Replacing the carbonyl moiety of the 3,4,5-trimethoxybenzoyl group of the compound **2a** with an oxygen atom furnished derivative **2b**. This compound was evaluated against the NCI 60 cell line panel and has an average IC_{50} value of 0.49 μM and an IC_{50} of 0.88 μM in the tubulin polymerization assay [25]. Compound **2c**, an analogue of derivative **2a**, is characterized by the presence of the 4′-methoxy-3′-hydroxyphenyl nucleus (corresponding to the B-ring of CA-4) at the 2-position of 3-(3,4,5-trimethoxybenzoyl)-benzo[*b*]thiophene skeleton [26]. While compound **2a** is a weak TPI, with $IC_{50} > 40$ μM, derivative **2c** is able to inhibit tubulin assembly with a IC_{50} of 3.5 μM. The two compounds **2a** and **2c** are also equipotent in inhibiting the growth of MCF-7 human breast carcinoma cells, with IC_{50} values of 0.64 and 0.52 μM, respectively, while compound **2c** is four-fold more potent than **2a** against human Burkitt lymphoma CA46 cells ($IC_{50} = 0.5$ and 2.0 μM, respectively). As with **2a**, derivative **2c** shows a modest inhibition (21%) of the binding of [^{3}H]colchicine to tubulin at a concentration of 5 μM. The activity of compounds **2a-c** appears to be highly dependent upon the presence of the 6-methoxy group on the benzo[*b*]thiophene ring.

In our work on anticancer agents based on the benzo[*b*]thiophene skeleton, we described a series of compounds based on the 2-alkoxycarbonyl-3-(3,4.5-trimethoxyanilino)-benzo[*b*]thiophene system, with 2-methoxy and 2-ethoxycarbonyl-3-(3,4,5-trimethoxyanilino)-6-methoxybenzo[*b*]thiophenes derivatives **2d** and **2e**, respectively. Both compounds display potent antiproliferative activity in the nanomolar range as inhibitors of the growth of cancer cell lines [27]. These compounds interact strongly with tubulin by binding to the colchicine site with activity comparable with that of CA-4. Although the presence of an ester function at the 2-position of the 3-(3,4,5-trimethoxyanilino)-6-methoxybenzo[*b*]thiophene system plays a pivotal role for potent antitumor activity, it represents a point of metabolic instability. Such esters can be degraded by human liver microsomes, arguing against the potential of this class of compounds as chemotherapeutic agents. This suggested the preparation of a new series of derivatives obtained by replacing the 2-alkoxycarbonyl group of compounds **2d-e** with the potentially more stable phenyl ring to overcome this potential metabolic instability.

We were intrigued by the idea of replacing the bridged carbonyl moiety of the 3,4,5-trimethoxybenzoyl group at the 3-position of the benzo[*b*]thiophene derivatives **2a** and **2c** with an anilinic nitrogen (NH) moiety to furnish a new series of 2-aryl-3-(3,4,5-trimethoxyanilino)-6-methoxybenzo[*b*]thiophene analogues with general structure **3** prepared by a flexible method, giving access to a wide range of substitution patterns at the 2-position of the 6-methoxybenzo[*b*]thiophene common

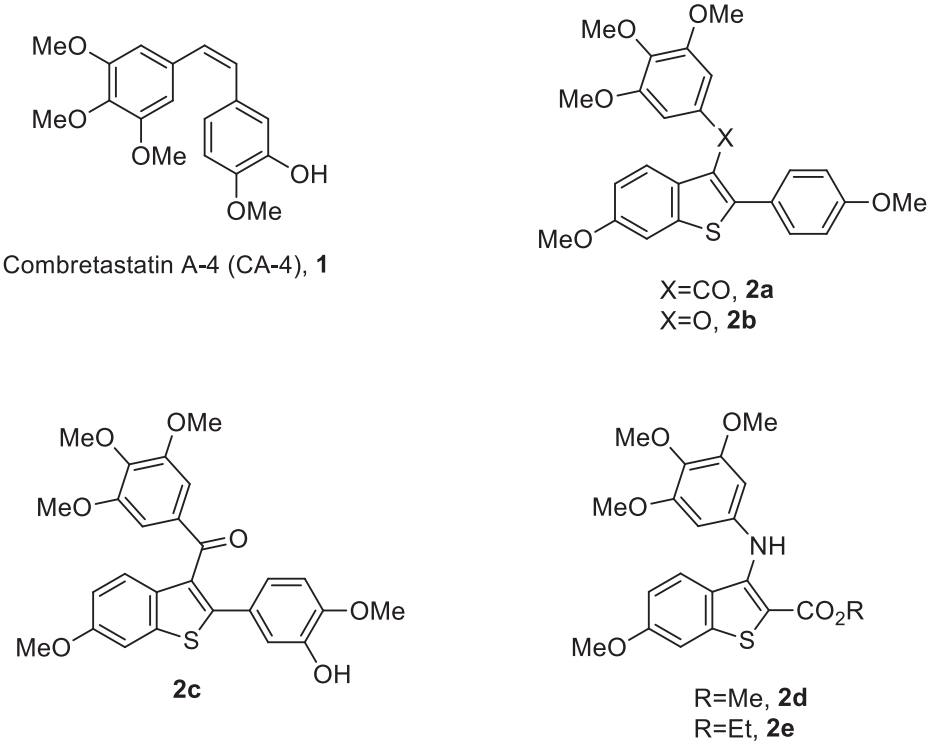

Fig. 1. Chemical structure of CA-4 (**1**) and representative examples of benzo[*b*]thiophene derivatives (**2a-e**).

intermediate (Fig. 2).

In the present study, all the synthesized compounds were characterized by a common 3-(3,4,5-trimethoxyanilino)-6-methoxybenzo[*b*]thiophene moiety, which characterized compounds **2d** and **2e**, and the modifications were focused on variation of the substituents on the phenyl ring located at the 2-position of the 3-(3,4,5-trimethoxybenzoyl/phenoxy)-6-methoxybenzo[*b*]thiophene derivatives **2a-c** (Fig. 2). Thus, once the 3-(3,4,5-trimethoxyanilino)-6-methoxybenzo[*b*]thiophene scaffold of compound **3p** was identified as the minimum structural requirement for activity in this series of compounds, our strategy for further development of active antimitotic agents was to perform modifications at the 2-position of the 6-methoxybenzo[*b*]thiophene ring. For compounds **3a-o**, the first attempt at optimization included the introduction of a phenyl ring at the 2-position of the benzo[*b*]thiophene molecular skeleton (compound **3a**). Modifications were also focused on varying the aryl moiety by adding electron-withdrawing (F) or electron-releasing (alkyl or alkoxy) groups at either the *para*- or *meta*-position of the 2-phenyl ring.

2. Chemistry

The 2-aryl-3-(3,4,5-trimethoxyanilino)-6-methoxybenzo[*b*]thiophene derivatives **3a-o** were synthesized by a three-step procedure shown in Scheme 1, starting from the common intermediate 6-methoxybenzo[*b*]thiophene **6**. This latter compound was synthesized by a two-step, previously reported procedure [28], starting from the commercially available 3-methoxybenzenethiol **4**, which, after *S*-alkylation with bromoacetaldehyde diethyl acetal to afford derivative **5**, was cyclicized with boron trifluoride etherate. Compound **6** was subjected to a regioselective C-2 arylation with different substituted iodobenzene derivatives [29], mediated by a catalytic amount of palladium (II) acetate in the presence of silver trifluoroacetate and trifluoroacetic acid as additives, in mild conditions with water as solvent with the addition of Tween 80 (2% w/w), to furnish derivatives **7a-o**.

The subsequent chemoselective C-3 bromination of compounds **7a-o** and derivative **6** with *N*-bromosuccinimide (NBS) in THF furnished the 2-aryl-3-bromo-6-methoxybenzo[*b*]thiophene derivatives **8a-o** and 3-

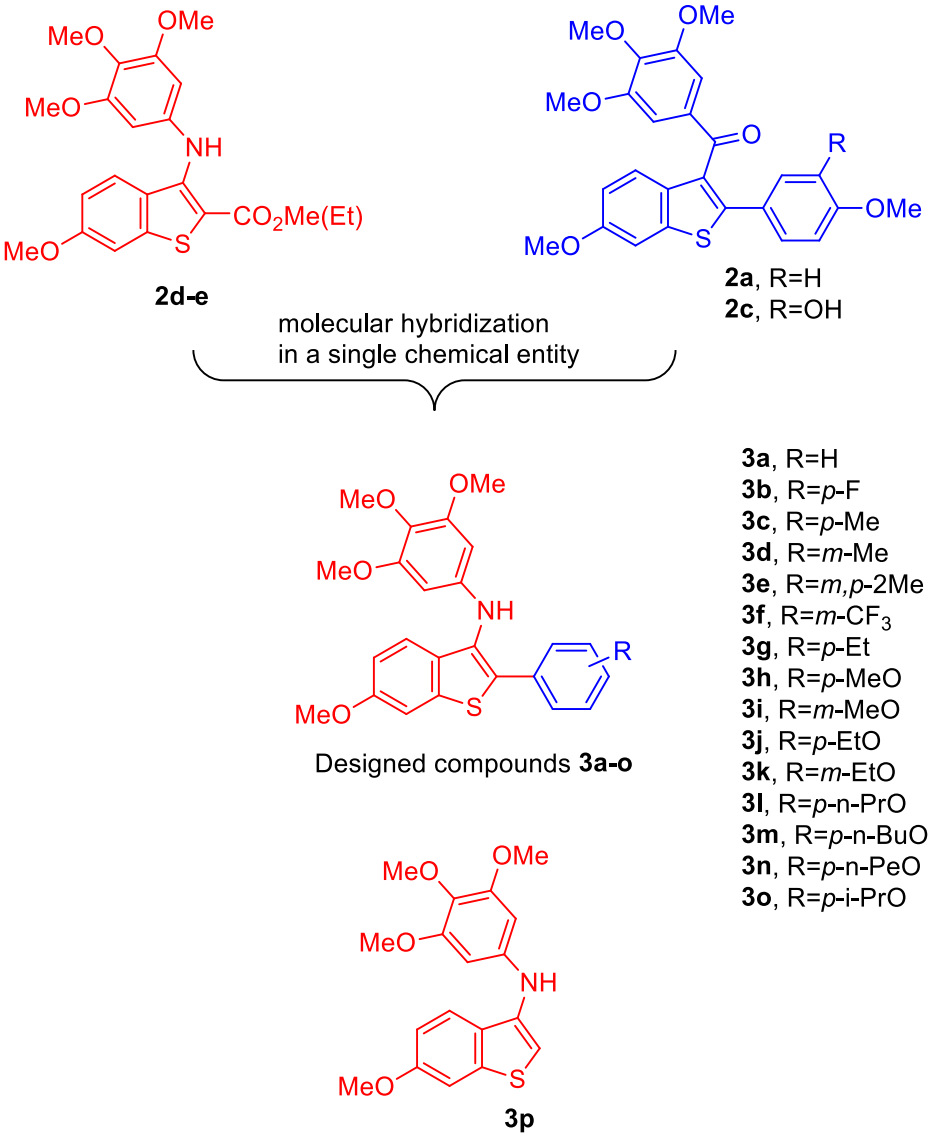

Fig. 2. Design strategy for conjugates **3a-p** obtained by the combination of pharmacophores of compounds **2a** and **2c-e**.

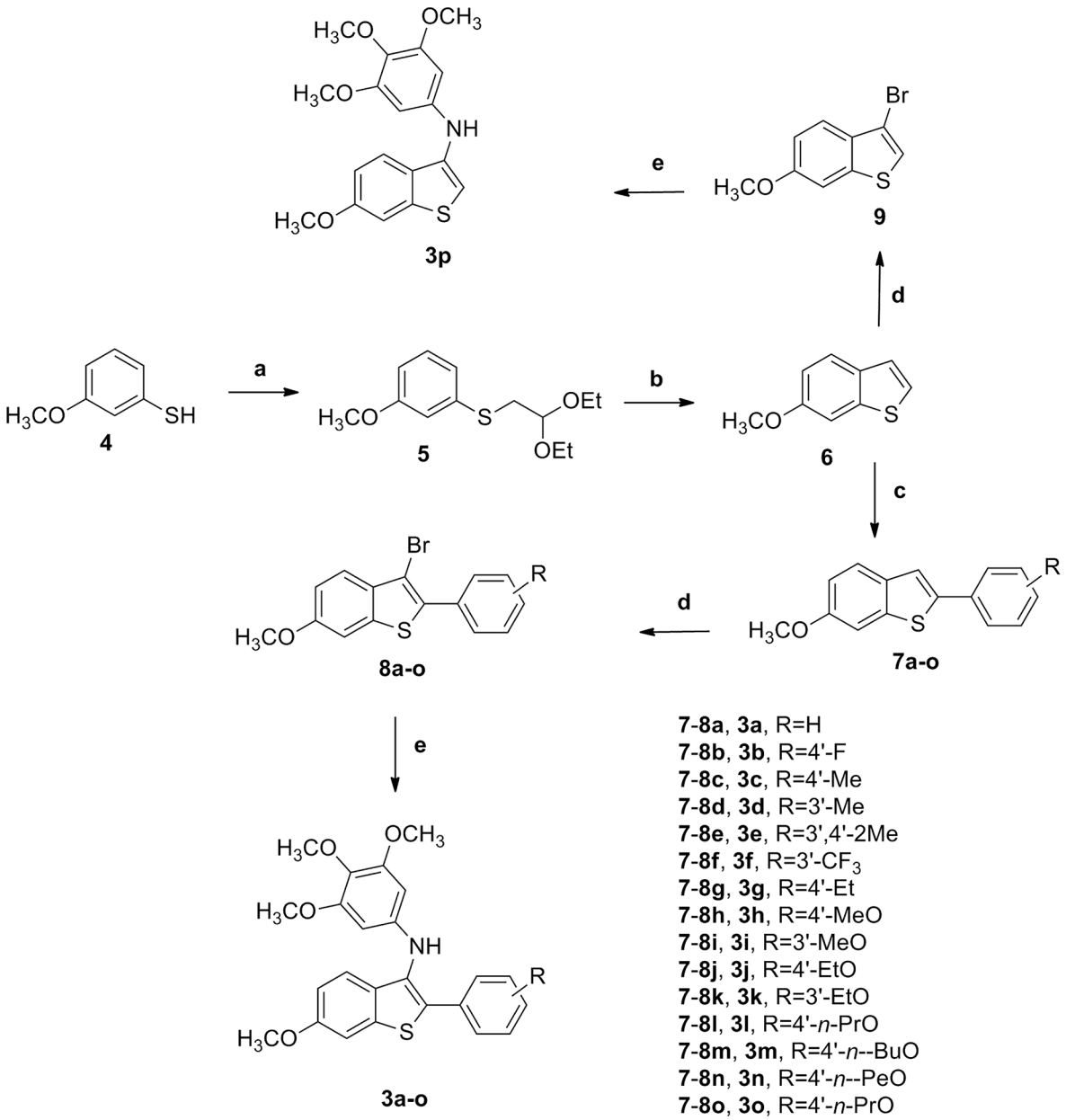

Scheme 1. Reagents and conditions. **a**: $BrCH_2CH(OEt)_2$, K_2CO_3, acetone, rt; **b**: BF_3 Et_2O, CH_2Cl_2, rt; **c**: ArI, $Pd(OAc)_2$ (5 mol%), CF_3COOAg, CF_3COOH, Tween 80/H_2O (2% w/w), rt, 48 h; **d**: NBS, THF; **e**: 3,4,5-trimethoxyaniline, Pd_2dba_3, xanthphos, sodium *t*-butoxide, toluene, 100 °C.

bromo-6-methoxybenzo[*b*]thiophene **9**, respectively. Finally, these latter compounds were submitted to the C—N Buchwald-Hartwig palladium catalyzed cross-coupling protocol, by reaction with 3,4,5-trimethoxyaniline in the presence of *tris*(dibenzylideneacetone)dipalladium(0) (Pd_2dba_3), 4,5-*bis*(diphenylphosphino)-9,9-dimethylxanthene (xanthphos) and sodium *tert*-butoxide (*t*-BuONa) (as catalyst, ligand and base, respectively) in toluene at 100 °C, to yield the novel derivatives **3a-p**.

3. Biological results and discussion

3.1. In vitro antiproliferative activities against human HeLa and HT-29 cell lines.

In Table 1, we summarize the growth inhibitory effects of the sixteen novel 3-(3,4,5-trimethoxyanilino)benzo[*b*]thiophene derivatives **3a-p** against the human cervix carcinoma (HeLa) and colon adenocarcinoma (HT-29) tumor cell lines, with CA-4 (**1**) as reference compound.

Compound **3a**, characterized by the presence of a phenyl ring at the 2-position of the 3-(3,4,5-trimethoxyanilino)-6-methoxybenzo[*b*]thiophene skeleton, was the most active compound of the series, with IC_{50} values of 0.23 and 0.06 μM against HeLa and HT-29 cancer cells, respectively. Although this derivative was less active than CA-4 against HeLa cells, it was very potent against the HT-29 cell line, which is resistant to CA-4, with an IC_{50} value of 60 nM. Along with compound **3a**, derivatives **3b** (*p*-F), **3c** (*p*-Me), **3 h** (*p*-OMe) and **3j** (*p*-OEt) were also more active than CA-4 against the HT-29 cell line. All the tested compounds were much less active than CA-4 against the HeLa cell line.

The substitution pattern on the phenyl moiety at the 2-position of the benzo[*b*]thiophene ring played an important role for antiproliferative activity. The introduction of the electron-withdrawing fluorine atom at the *para*-position of the 2-phenyl ring (**3b**) led to a 2- and 7-fold

Table 1
In vitro inhibitory effects of compounds **3a-p** and reference derivative CA-4 (**1**) on proliferation of HeLa and HT-29 human tumor cell lines.

Compound	IC_{50} (μM)	
	HeLa	HT-29
3a	0.23 ± 0.05	0.06 ± 0.03
3b	0.5 ± 0.05	0.4 ± 0.05
3c	0.5 ± 0.04	1.4 ± 0.7
3d	21.5 ± 3.1	12.0 ± 2.0
3e	11.0 ± 2.3	9.2 ± 2.7
3f	26.7 ± 0.9	25.7 ± 1.2
3 g	14.1 ± 3.2	5.6 ± 1.1
3 h	1.5 ± 0.05	1.7 ± 07
3i	8.2 ± 2.1	6.2 ± 0.7
3j	1.8 ± 03	1.0 ± 0.2
3 k	30.1 ± 1.2	36.0 ± 2.6
3 l	37.1 ± 3.3	16.6 ± 0.5
3 *m*	18.9 ± 2.3	7.9 ± 05
3*n*	28.3 ± 2.2	21.0 ± 0.7
3o	22.9 ± 3.6	12.9 ± 5.0
3p	1.7 ± 0.2	6.2 ± 0.9
CA-4 (1)	0.004 ± 0.001	3.1 ± 0.1

[a]IC_{50} = compound concentration required to inhibit tumor cell proliferation by 50%. Data are expressed as the mean ± SE from the dose–response curves of at least three independent experiments carried out in triplicate.

reduction in activity against HeLa and HT-29 cells, respectively, in comparison with the parent unsubstituted 2-phenyl analogue **3a**. Derivative **3b,** with IC_{50} values of 0.5 and 0.4 μM, against HeLa and HT-29 cells, respectively, along with compound **3a**, were the only compounds of the series active at sub-micromolar concentrations against both cancer cell lines. Replacing fluorine with the weak-electron releasing methyl group, to furnish derivative **3c**, yielded a compound that maintained activity against HeLa cells but that had 3.5-fold reduced potency against HT-29 cells. Moving the methyl group from the *para*- to the *meta*-position had a negative effect in maintaining antiproliferative activities, with the *meta*-tolyl derivative **3d** 43- and 9-fold less active than the isomeric *para*-tolyl **3c** against HeLa and HT-29 cells, respectively. Replacement of the methyl moiety of **3d** with the strong electron-withdrawing trifluoromethyl group, to furnish derivative **3f**, maintained the antiproliferative activity on HeLa cells and caused a 2-fold reduction in potency on HT-29 cells. Starting from compound **3c**, homologation of the alkyl chain from methyl to ethyl (to yield derivative **3 g**) had a detrimental effect on activity, with a 28- and 4-fold reduction of potency relative to **3c** on HeLa and HT-29 cells, respectively. A similar reduction in activity was observed with an additional methyl group at the *meta*-position of *para*-tolyl derivative **3c**, to furnish the *meta*, *para*-xylyl analogue **3e**.

Replacing the weak electron-releasing methyl with the stronger methoxy group at the *para* position of the 2′-phenyl group (to furnish compound **3 h**) caused a 3-fold reduction in activity against HeLa cells, while the two compounds had similar potency against HT-29 cells. Moving the methoxy group from the *para*- to the *meta*-position (compounds **3 h** and **3i**, respectively) caused a 5- and 4-fold reduction in activity against HeLa and HT-29 cells, respectively, a reduction that was less dramatic than that observed for the two isomeric *para*- and *meta*-tolyl derivatives **3c** and **3d**.

Unlike what was observed for the *para*-methyl and ethyl homologues **3c** and **3 g**, respectively, increasing the length of the alkoxy chain from *para*-methoxy (**3i**) to ethoxy (**3j**) resulted in a 2-fold increase in antiproliferative activity against HT-29 cells, while the two compounds were equipotent against HeLa cells. A dramatic drop of activity (17- and 36-fold against HeLa and HT-29 cells, respectively) was observed by moving the ethoxy group from the *para*- to the *meta*-position (derivatives **3j** and **3 k**, respectively). Starting from *para*-ethoxy derivative **3j**, a further homologation of the alkyl chain of the alkoxy moiety from ethyl to *n*-propyl (**3 l**) to *n*-butyl (**3 m**) to end with *n*-pentyl (**3n**) or the presence of branched isopropyl chain (**3o**) at the *para*-position of the phenyl ring was not tolerated, being detrimental for antiproliferative activity, with 10–20- and 8–36-fold reduction of activity against HeLa and HT-29 cells, respectively, relative to compound **3j**. These compounds thus revealed the importance of the steric effect of the substituent at the *para*-position of the 2′-phenyl on antiproliferative activity

Finally, removing the 2-phenyl group of compound **3a**, to furnish derivative **3p**, caused a 7- and 100-fold reduction of activity against HeLa and HT-29 cells, respectively, thus demonstrating that the presence at the 2-position of the 3-(3,4,5-trimethoxyanilino)-6-methoxybenzo[*b*]thiophene molecular skeleton of a phenyl group without substituents or with a small electronegative fluorine atom at its *para*-position (derivatives **3a** and **3b**, respectively) was essential for potent antiproliferative activity, while the introduction of electron-releasing alkyl or alkoxy substituents was not as well tolerated and reduced potency. Moreover, the position of the substituent on the phenyl ring influenced antiproliferative activity, with the *p*-substituted phenyl derivatives **3c** (methyl), **3 h** (methoxy) and **3j** (ethoxy) being more potent than the isomeric *m*-substituted phenyl analogues **3d**, **3i** and **3 k**, respectively.

3.2. Molecular modeling studies

To evaluate the influence of the new structural modifications that characterize compounds with general structure **3** on binding in the colchicine site of αβ-tubulin, preliminary docking studies were performed. There was significant overlap with the co-crystallized colchicine, with the trimethoxyphenyl ring in proximity to βCys241, a key interaction point for tubulin polymerization inhibition (Fig. 3A, 2-(4-fluorophenyl)-3-(3,4,5-trimethoxyanilino)-6-methoxybenzo[*b*]thiophene derivative **3b**). The benzo[*b*]thiophene portion pointed towards the tubulin α-subunit, with the sulfur atom interacting with βLys352 and at an optimal distance of 3.1 Å, permitting an interaction with atoms of the polypeptide backbone of αThr179. The differently *para*-substituted phenyl rings could be tolerated and are placed in a small hydrophobic area near βMet259, where the colchicine methoxy group is positioned, and the latter is involved in different interactions than the former with the surrounding residues. Interestingly, all the docked derivatives occupy the colchicine site in a comparable manner (Fig. 3B, 2-(4-ethoxyphenyl)-3-(3,4,5-trimethoxyanilino)-6-methoxybenzo[*b*]thiophene derivative **3j**). The potential binding mode for this new family of compounds, as determined in molecular modeling studies, was consistent with an interaction at the colchicine site. To prove this hypothesis, selected compounds were tested for their *in vitro* inhibitory activities both of tubulin assembly and colchicine binding to tubulin.

3.3. In vitro inhibition of tubulin polymerization and colchicine binding

To investigate whether the antiproliferative activities of the most potent compounds of the series derived from an interaction with microtubules, derivatives **3a-c**, **3h** and **3j** were selected to determine their ability to inhibit tubulin polymerization and for effects on the binding of [^{3}H]colchicine to tubulin. For comparison, CA-4 was examined in contemporaneous experiments and strongly inhibited tubulin polymerization with an IC_{50} value of 0.54 μM. In contrast to the molecular modeling studies reported in the introduction section that predicted that these compounds should be characterized by an excellent affinity in the binding site of colchicine in tubulin, none of the compounds examined significantly affected tubulin assembly, as all had an $IC_{50} > 20$ μM. Moreover, in the colchicine binding studies, only modest inhibition (30%) of the binding of [^{3}H]colchicine to tubulin was observed with 5 μM compound **3b**, in comparison with CA-4, which in these experiments inhibited colchicine binding by 97%. Inhibition of colchicine binding by derivatives **3a**, **3c**, **3 h** and **3j** was even lower (7–24% inhibition was observed with these agents).

The results of the *in vitro* inhibition of tubulin polymerization and colchicine-binding assays did not support the preliminary data of the

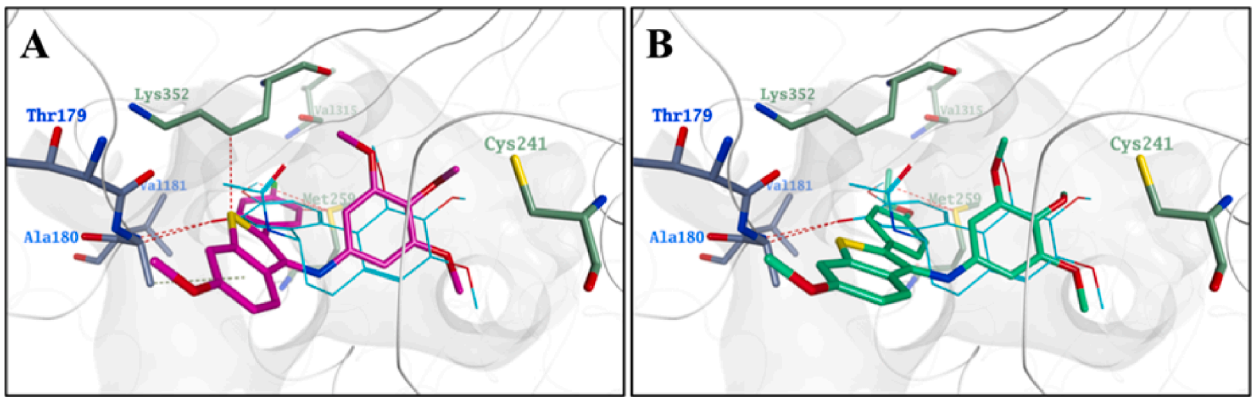

Fig. 3. A) Proposed binding for compound **3b** in the colchicine site. The trimethoxyphenyl ring is in proximity to βCys241, while the benzo[*b*]thiophene portion is pointing towards the tubulin α-subunit. The *p*-fluoro phenyl ring is placed in a small hydrophobic area near βMet259. B) Proposed binding mode for **3j**. In both panels, co-crystallized colchicine is shown in cyan, and the carbon atoms of α-tubulin residues are shown in blue, those of the β-subunit are in dark green. (For interpretation of the references to colour in this figure legend, the reader is referred to the web version of this article.)

computational-based docking studies reported in the previous section and are consistent with the conclusion that the tested compounds may exert their antiproliferative effects by mechanisms other than inhibition of tubulin assembly at the colchicine site. In this regard, replacing the sp^2 centre of the carbonyl in the 3,4,5-trimethoxybenzoyl moiety of derivatives **2a** and **2c** with an anilinic nitrogen (NH) reduced anti-tubulin activity.

*3.4. Antitumoral properties of compounds **3a** and **3b** in colorectal cancer cells*

Because of their initial activity in HT-29 colon cancer cells, we examined the effects of **3a** and **3b** in other colon cell lines. This seemed pertinent because of the major impact of colorectal cancer on human health. In 2019, the Global Cancer Observatory (GLOBOCAN) reported colorectal cancer as the second most deadly and the third most common cancer diagnosed in the world [30]. For this reason, and taking into consideration the promising antiproliferative activities of compounds **3a** and **3b** in HT-29 cells, we undertook an in-depth analysis of their *in vitro* effects on three different types of colon cells: Caco2 (not metastatic), HCT-116 (metastatic) and 841 CoN (non-tumor cells), all with epithelial-like morphology. In most of the following studies, we used the IC_{50} values obtained with the HT-29 cells (60 nM for **3a** and 400 nM for **3b**).

*3.4.1. Derivatives **3a** and **3b** trigger apoptotic cell death*

First, we investigated the ability of compounds **3a** and **3b** to induce apoptotic cell death, as cancer cells are significantly more resistant to apoptotic stimuli than are non-transformed cells [31]. The three cell lines (Caco2, HCT-116 and 841 CoN) were treated with 60 nM **3a** or 400 nM **3b** for 48 h, and these treatments triggered a significant induction of apoptosis as suggested by the increased expression of cleaved poly(ADP-ribose) polymerase (PARP), receptor-interacting protein (RIP) and caspase 3 proteins and by the intensity of annexin-V staining in both metastatic and non-metastatic cells (Fig. 4A and 4B). Not to be underestimated in anticancer strategies are the side effects of drugs in the "healthy" cells surrounding the cancer cells [32]. Thus, the same analyses were performed on non-transformed 841 CoN cells. These cells showed no differences between vehicle and **3a** and **3b** treatments, highlighting the absence of apoptotic effects on normal cells following a therapeutic treatment with compound **3a** or **3b** (Fig. 4A and 4B).

*3.4.2. Compounds **3a** and **3b** induce cell cycle arrest*

Cancer cells almost always display abnormalities in the control of cell cycle checkpoints, and thus strategies able to affect this process are crucial for counteracting tumor growth [33]. To investigate whether compounds **3a** and **3b** affected cell cycle progression, and thus proliferation, two important assays were performed. First, we measured the percentages of cells in the G0/G1, S and G2/M phases, via fluorescence and propidium iodide (PI) incorporation (which quantifies cellular DNA content); the second and more specific assay explored the expression of key proteins involved in the cell cycle, such as cyclins (Cyc.), p27 (marker of G1 phase) and pHH3 (marker of mitosis). The first method unveiled a strong effect of **3a** and **3b** in Caco2 and HCT-116 cells concerning cell accumulation in the G0/G1 phase, but not the G2/M phase, without any appreciable effects on 841 CoN cells (Fig. 5A). The second

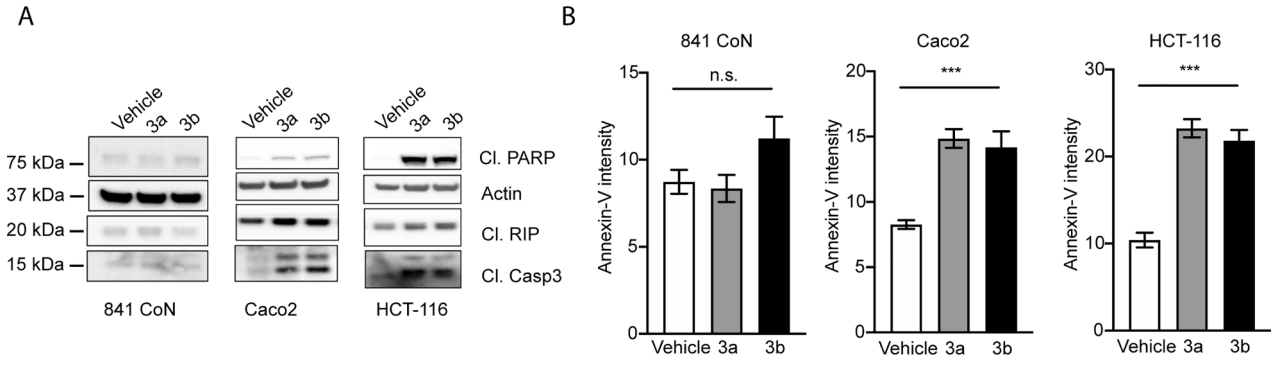

Fig. 4. (A) Cleaved PARP, RIP and caspase 3 protein expression evaluated to determine the extent of cell death occurring in the Caco2 and HCT-116 cell lines, but not in 841 CoN cells, following treatment with **3a** or **3b**. (B) Detection of apoptosis by annexin-V staining quantification in 841 CoN, Caco2 and HCT-116 cell lines following **3a** (grey bar) or **3b** (black bar) treatment at 60 or 400 nM, respectively. N.s. = not significant; *** = $p < 0.001$.

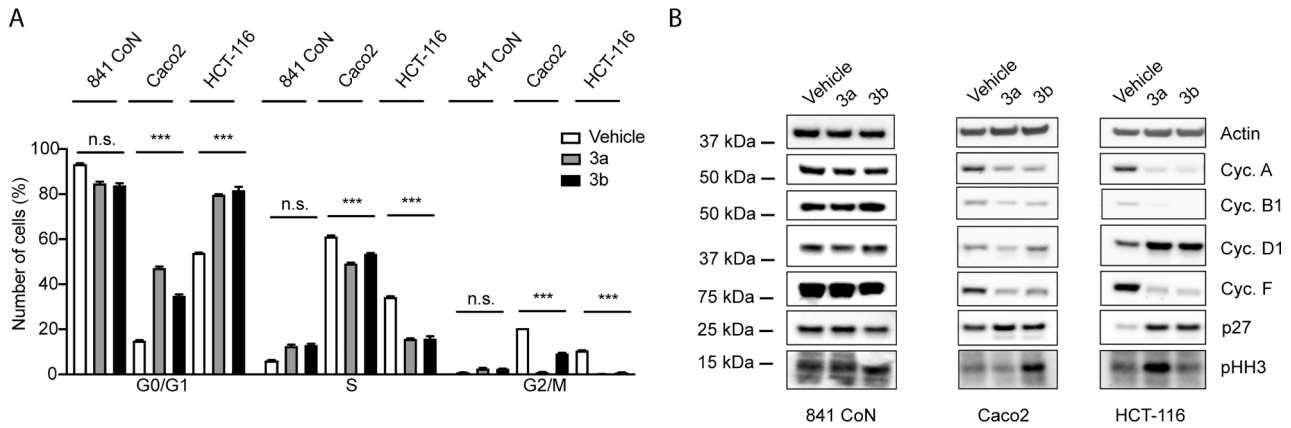

Fig. 5. (A) Calculation in percentage of the amount of 841 CoN, Caco2 and HCT-116 cells in G0/G1, S and G2/M phases in basal condition and after **3a** (grey bar) or **3b** (black bar) treatments at 60 or 400 nM, respectively, on the basis of the PI uptake. (B) Cell cycle marker investigation under the same conditions as were used in Panel A by using selective antibodies against markers of the cell cycle: Cyc. D1 and p27 for G1 phase; Cyc. A for S phase; Cyc. F and B1 for G2/M; pHH3 for mitosis. Cyc. = Cyclin; n.s. = not significant; *** = $p < 0.001$.

assay confirmed the preliminary data obtained in Fig. 5A, showing increased expression of G1 phase markers (in accord with the cell accumulation in G1), such as Cyc. D1 and p27 for both the compounds in HCT-116 and Caco2 cells, and a concomitant decrease of proteins involved in the S (Cyc. A) and G2/M (Cyc. B1 and F) phases (Fig. 5B). The cell cycle marker evaluation revealed also a significant accumulation of pHH3 in Caco2 following **3b** administration and in HCT-116 for **3a**, not detected by the previous method. These findings not only confirmed cell cycle arrest in G1 phase, but also indicated a potential additional effect during mitosis for **3a** in metastatic cells and for **3b** in non-metastatic cells (Fig. 5B). Also, in this case, no effects were detected in the 841 CoN control cells.

3.4.3. *Derivatives **3a** and **3b** impact mitochondrial morphology and mitochondrial dynamics*

Mitochondria, organelles of bacterial origin and responsible for producing energy for the whole body, are physically and functionally associated with the intrinsic apoptotic pathway that often is disrupted during cancer cell transformation [34,35]. Therefore, we evaluated several mitochondrial parameters that might have been altered as a

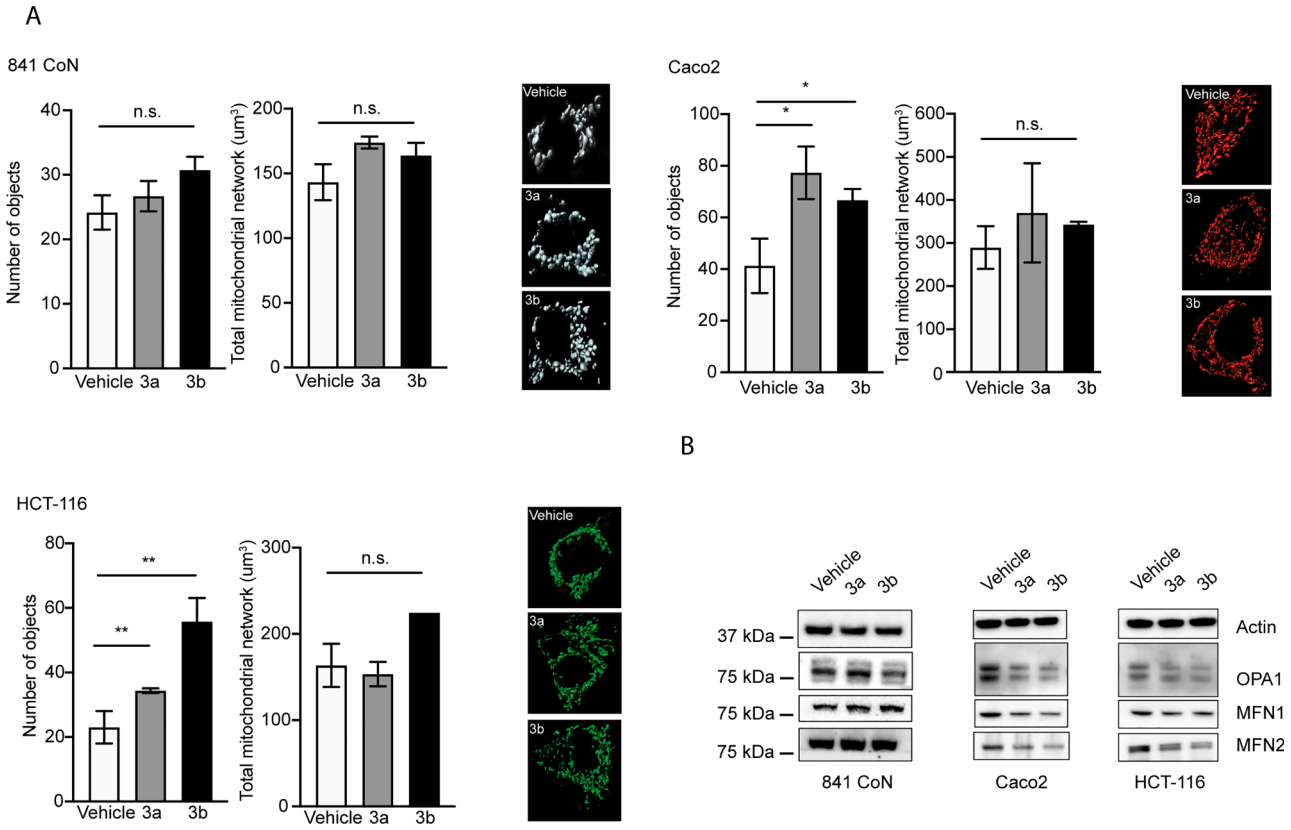

Fig. 6. (A) Mitochondrial morphology investigation. Representative images in 841 CoN, Caco2 and HCT-116 cells using the mtDSRed plasmid. Number of objects index shows the number of mitochondria inside cells in each experimental condition, and the volume of the total mitochondrial network is quantitated in terms of μ^3. (B) Evaluation of the expression of proteins involved in mitochondria fusion (OPA1, MFN1 and MFN2). Reaction conditions were as used in the experiments shown in Panel A. For Panel A: n.s. = not significant; * = $p < 0.05$; ** = $p < 0.01$; *** = $p < 0.001$.

consequence of the apoptotic process.

Current opinion is that mitochondrial fragmentation occurs during apoptosis, yielding an increased number of smaller and dysfunctional mitochondria [36]. To determine whether **3a** and **3b** caused this effect while they induced apoptosis, we examined mitochondrial morphology with the mitochondria-targeted red fluorescent protein mtDsRed, which was transfected into cells in the same manner in all experimental conditions. Cells were treated with **3a** or **3b** at 60 or 400 nM, respectively, and images of treated, living cells (HCT-116 and Caco2) demonstrated increased numbers of mitochondria (designated as n° of objects), without changes in the total mitochondrial network (Fig. 6A) when compared to untreated cells. As a consequence, mitochondria appeared smaller following compound treatment, in terms of the volume of an individual mitochondrion. In nontumoral cells, no appreciable changes were detected. Taken together, these findings indicated a significant organelle fragmentation following **3a** or **3b** treatment without changes in the overall mitochondrial mass.

Moreover, mitochondria are dynamic structures that fuse and divide continuously [36,37]. This phenomenon is ensured by a pool of GTPase proteins with a prevalent mitochondrial localization. In humans, these proteins include Mfn1, Mfn2 and Opa1, and they are involved in mitochondrial fusion events. To understand the cause of mitochondrial fragmentation, we tested OPA1, MFN1 and MFN2 expression levels before and after treatments with **3a** or **3b** (Fig. 6B). In agreement with the morphology findings, the 841 CoN colon cells did not show any change in protein expression, in contrast to the two colon cancer cell lines, where their expression was reduced (Fig. 6B). These data demonstrated that **3a** and **3b** induced mitochondrial fragmentation by reducing expression of proteins that ensure mitochondrial fusion.

3.4.4. *Derivatives **3a** and **3b** impact mitochondrial membrane potential*

Dissipation of mitochondrial membrane potential is an early event of apoptosis, and we therefore measured it by the tetramethylrhodamine methyl ester (TMRM) probe. Treatment of cells with **3a** or **3b** led to a significant reduction of mitochondrial potential when compared to the untreated condition (Fig. 7A). In the control 841 CoN cells, compound **3a** did not affect mitochondrial membrane potential, but **3b** showed a negative effect (Fig. 7A).

3.4.5. *Mitochondrial calcium handling*

Mitochondria are organelles that exert most of their functions by controlling intracellular calcium, which is derived either from such internal stores as the endoplasmic reticulum or from the extracellular milieu [34,38]. Increased mitochondrial calcium uptake may be a signal for cell death via the intrinsic pathway [39]. We therefore measured mitochondrial calcium homeostasis using a specific organelle-target aequorin (AEQ) probe, one targeted to mitochondria (mtAEQ). First, we transfected mtAEQ into 841 CoN, Caco2 and HCT-116 cells, and, second, we treated them with vehicle or compound **3a** or **3b**. Under all conditions we investigated, the ATP agonist caused a significant increase in calcium uptake only in the metastatic HCT-116 cell line following **3a** or **3b** treatment. No differences were detected in the control 841 CoN or non-metastatic Caco2 cells (Fig. 7B).

4. Conclusions

Previously [27], we discovered a new class of structurally simple synthetic inhibitors of tubulin polymerization, based on the 3-(3,4,5-trimethoxyanilino)-6-methoxybenzo[*b*]thiophene moiety of compounds with general structure **2d-e**. Here, we have synthesized a new series of related compounds in a concise three-step synthetic procedure starting from a 6-methoxybenzo[*b*]thiophene common intermediate. Modifications were focused on varying the aryl moiety at the C-2 position of the 6-methoxybenzo[*b*]thiophene nucleus by adding electron-withdrawing (F) or electron-releasing (Me, Et and alkoxy) groups The 2-phenyl-3-(3,4′5-trimethoxyanilino)-6-methoxybenzo[*b*]thiophene derivative **3a** displayed the greatest antiproliferative activity among the new compounds, with IC_{50} values of 0.23 and 0.06 μM against HeLa and HT-29 cells, respectively. We observed that the insertion of a substituent at the *para*-position of the phenyl at the 2-position of the 6-methoxybenzo[*b*]thiophene nucleus reduced antiproliferative activity in comparison with the unsubstituted phenyl analogue **3a**. This effect was less pronounced by the introduction of an electron-withdrawing fluorine atom (compound **3b**), and it was more evident for electron releasing alkyl and alkoxy groups, suggesting that the presence of the unsubstituted phenyl moiety at the 2-position of 6-methoxybenzo[*b*]thiophene nucleus was best for antiproliferative activity. Five of the synthesized compounds, **3a**, **3b** (*p*-F), **3c** (*p*-Me), **3 h** (*p*-OMe) and **3j** (*p*-OEt), had the best antiproliferative activities against the CA-4 resistant HT-29 cell line and were 3–50-fold more active than CA-4. Mechanism studies demonstrated that **3a** and **3b** arrested cell cycle progression predominantly in the G0/G1 phase and induced cell apoptosis. Although molecular modeling studies predicted that these compounds could act through inhibition of tubulin polymerization, fitting well into the colchicine site, the *in vitro* assays demonstrated that for the most active derivatives antiproliferative activity was not related to inhibition of tubulin assembly. This was also confirmed based on the failure to observe the usual G2/M arrest with either **3a** or **3b**. For all these reasons, we think it unlikely that tubulin plays a significant role in the cytotoxicity of these compounds, especially in view of their weak inhibition of colchicine

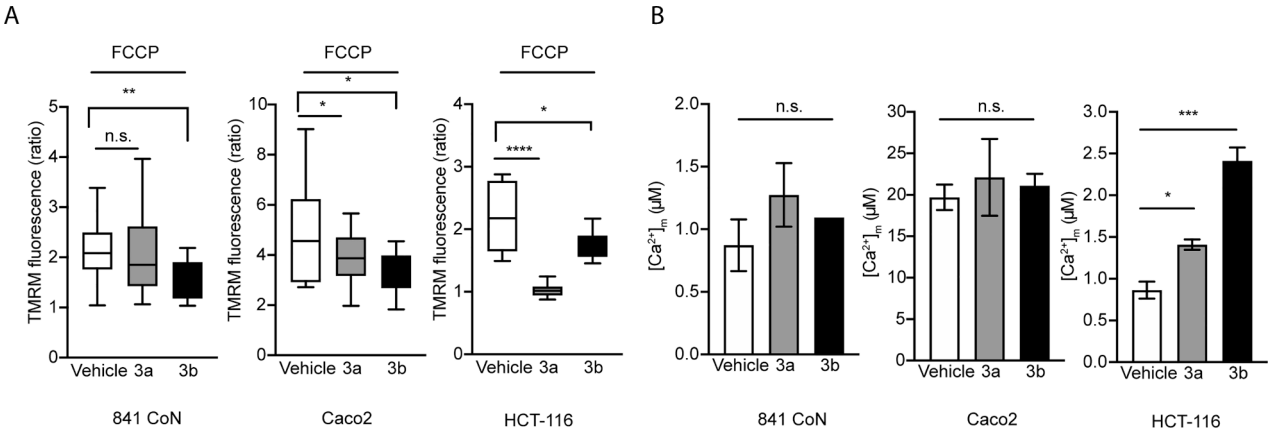

Fig. 7. (A) Mitochondrial membrane potential in 841 CoN, Caco2 and HCT-116 cells measured by using the TMRM probe. Values on the ordinate are expressed as arbitrary fluorescence ratio between TMRM fluorescence in basal conditions and upon FCCP administration. (B) Mitochondrial calcium uptake upon agonist (ATP) administration measured by transfecting cells with the luminescent mitochondria-targeted aequorin. Reaction conditions were the same as used in the experiments shown in Panel A. n.s. = not significant; * = $p < 0.05$; ** = $p < 0.01$; *** = $p < 0.001$.

binding.

The good activity of several derivatives in the HT-29 colon cancer cells led us to perform a detailed analysis in two additional colon cancer cell lines and in a non-transformed colon cell line. These studies confirmed the antiproliferative properties of compounds **3a** and **3b** against colon cancer cells and showed that the compounds strongly induced cell death and cell cycle arrest in the G0/G1 phase. Our data demonstrated that apoptosis was a mechanism of cell death, but other types of cell death cannot yet be excluded. As apoptosis can be triggered by the intrinsic pathway, we explored the "state of health" of the mitochondrial pool by measuring the morphology, membrane potential and calcium homeostasis of mitochondria following **3a** and **3b** treatment. Both derivatives triggered mitochondrial fragmentation by negatively modulating OPA1, MFN1 and MFN2, and they lowered mitochondrial membrane potential. We observed that these effects occurred in the two colon cancer cell lines, but not in the non-transformed 841 CoN colon cells. Thus, based on these *in vitro* findings, **3a** and **3b** could be considered as safe for the tumor-surrounding healthy tissues as they had no or limited effects on 841 CoN control colon cells. In these cells, our only negative finding was a loss of mitochondrial membrane potential with **3b** treatment, perhaps indicating toxicity with prolonged treatment. A second issue concerns possible differential affinities towards metastatic and non-metastatic tumors. Derivatives **3a** and **3b** showed greater effectiveness for HCT-116 cells, which displayed a greater extent of cell death and decrease in mitochondrial membrane potential as compared with the non-metastatic Caco2 cells. Moreover, **3a** and **3b** caused increased calcium uptake in mitochondria, an important signal of cell death, in HCT-116 cells but not in Caco2 cells. A further difference between the two colon cancer cell lines was an additional block in mitosis caused by **3a** (but not **3b**) in HCT-116 cells and by **3b** (but not **3a**) in Caco2 cells. Further studies of the molecular mechanism of action of **3a** and **3b** are underway.

5. Experimental protocols

5.1. Chemistry

5.1.1. Materials and methods

^{1}H experiments were recorded on either a Bruker AC 200 or a Bruker Avance III 400 spectrometer, and ^{13}C NMR spectra were recorded on a Varian 400 Mercury Plus or a Bruker Avance III 400 spectrometer. Chemical shifts (δ) are given in ppm upfield, and the spectra were recorded in appropriate deuterated solvents, as indicated. Mass spectra were recorded by an ESI single quadrupole mass spectrometer Waters ZQ 2000 (Waters Instruments, UK), and the values are expressed as $[M + 1]^+$. Melting points (mp) were determined on a Buchi-Tottoli apparatus and are uncorrected. All products reported showed ^{1}H and ^{13}C NMR spectra in agreement with the assigned structures. The purity of tested compounds was determined by combustion elemental analyses conducted by the Microanalytical Laboratory of the Chemistry Department of the University of Ferrara with a Yanagimoto MT-5 CHN recorder elemental analyzer. All tested compounds yielded data consistent with a purity of at least 95% as compared with the theoretical values. Reaction courses and product mixtures were routinely monitored by TLC on silica gel (precoated F_{254} Merck plates), and compounds were visualized with aqueous $KMnO_4$. Flash chromatography was performed using 230–400 mesh silica gel and the indicated solvent system. Organic solutions were dried over anhydrous Na_2SO_4.

5.1.2. General procedure a for the synthesis of compounds *7a-o*

To a suspension of 6-methoxybenzo[*b*]thiophene **6** (164 mg, 1 mmol), CF_3COOAg (331 mg, 1.5 mmol), trifluoroacetic acid (228 mg, 0.15 mL, 2 mmol), the appropriate iodobenzene derivative (2.0 mmol) and Tween-80/H_2O (2 mL, 2 wt%) was degassed under a stream of argon over 10 min. $Pd(OAc)_2$ (11.2 mg, 0.05 mmol, 5 mol %) was added and the mixture degassed again for 10 min, then stirred at room temperature for 48 h. After this time, the reaction mixture was diluted with EtOAc (10 mL), filtered on a pad of celite and the filtrate washed sequentially with water (5 mL) and brine (5 mL), dried over Na_2SO_4 and evaporated under reduced pressure. The crude residue was purified by flash column chromatography on silica gel using a mixture of ethyl ether and petroleum ether to afford the title compound.

*5.1.2.1. 6-Methoxy-2-phenylbenzo[b]thiophene (**7a**).* Following general procedure A, the crude residue purified by flash chromatography, using Et_2O:petroleum ether 0.5:9.5 (v:v) for elution, furnished compound **7a** as a yellow oil. Yield: 75%. ^{1}H NMR (DMSO-d_6) δ: 3.84 (s, 3H), 7.04 (dd, J = 9.0 and 2.4 Hz, 1H), 7.41 (dd, J = 8.6 and 1.8 Hz, 1H), 7.48–7.51 (m, 1H), 7.54–7-62 (m, 2H), 7.60–7.62 (m, 2H), 7.64 (d, *J* = 2.4 Hz, 1H), 7.73 (d, *J* = 9.0 Hz, 1H). MS (ESI): $[M + 1]^+$=241.3.

*5.1.2.2. 2-(4-Fluorophenyl)-6-methoxybenzo[b]thiophene (**7b**).* Follow ing general procedure A, the crude residue purified by flash chromatography, using petroleum ether for elution, furnished compound **7b** as a white solid. Yield: 62%, mp 63 °C. ^{1}H NMR (DMSO-d_6) δ: 3.84 (s, 3H), 7.03 (dd, J = 9.0 and 2.4 Hz, 1H), 7.29–7.39 (m, 4H), 7.59–7.66 (m, 2H), 7.69 (d, *J* = 9.0 Hz, 1H). MS (ESI): $[M + 1]^+$=259.3.

*5.1.2.3. 6-Methoxy-2-(p-tolyl)benzo[b]thiophene (**7c**).* Following general procedure A, the crude residue purified by flash chromatography, using Et_2O:petroleum ether 0.1:9.9 (v:v) for elution, furnished compound **7c** as a colorless oil. Yield: 85%. ^{1}H NMR (DMSO-d_6) δ: 2.40 (s, 3H), 3.82 (s, 3H), 6.97 (dd, J = 8.8 and 2.4 Hz, 1H), 7.33–7.38 (m, 6H), 7.61 (d, *J* = 2.4 Hz, 1H). MS (ESI): $[M + 1]^+$=255.3.

5.1.2.4. 6-Methoxy-2-(m-tolyl)benzo[b]thiophene (7d). Following general procedure A, the crude residue purified by flash chromatography, using Et_2O:petroleum ether 0.1:9.9 (v:v) for elution, furnished compound **7d** as a colorless oil. Yield: 58%. ^{1}H NMR (DMSO-d_6) δ: 2.39 (s, 3H), 3.84 (s, 3H), 7.04 (dd, J = 9.0 and 2.4 Hz, 1H), 7.21–7.24 (m, 2H), 7.36–7.41 (m, 2H), 7.57 (s, 1H), 7.63 (d, *J* = 2.4 Hz, 1H), 7.73 (d, *J* = 8.8 Hz, 1H). MS (ESI): $[M + 1]^+$=255.3.

*5.1.2.5. 2-(3,4-Dimethylphenyl)-6-methoxybenzo[b]thiophene (**7e**).* Following general procedure A, the crude residue purified by flash chromatography, using petroleum ether for elution, furnished compound **7e** as a colorless oil. Yield: 56%. ^{1}H NMR (DMSO-d_6) δ: 2.82 (s, 3H), 2.98 (s, 3H), 3.84 (s, 3H), 7.01 (dd, J = 8.8 and 2.4 Hz, 1H), 7.27–7.32 (m, 3H), 7.51 (s, 1H), 7.62 (d, *J* = 2.4 Hz, 1H), 7.72 (d, *J* = 8.8 Hz, 1H). MS (ESI): $[M + 1]^+$=269.4.

*5.1.2.6. 6-Methoxy-2-(3-(trifluoromethyl)phenyl)benzo[b]thiophene (**7f**).* Following general procedure A, the crude residue purified by flash chromatography, using Et_2O:petroleum ether 0.1:9.9 (v:v) for elution, furnished compound **7f** as a colorless oil. Yield: 53%. ^{1}H NMR (DMSO-d_6) δ: 3.85 (s, 3H), 7.11 (dd, J = 8.8 and 2.4 Hz, 1H), 7.67 (d, *J* = 2.6 Hz, 1H), 7.70 (d, *J* = 8.8 Hz, 1H), 7.77–7.80 (m, 3H), 7.87–7.94 (m, 2H). MS (ESI): $[M + 1]^+$=309.3.

*5.1.2.7. 2-(4-Ethylphenyl)-6-methoxybenzo[b]thiophene (**7g**).* Following general procedure A, the crude residue purified by flash chromatography, using petroleum ether for elution, furnished compound **7 g** as a colorless oil. Yield: 53%. ^{1}H NMR (DMSO-d_6) δ: 1.23 (t, *J* = 7.6 Hz, 3H), 2.65 (q, *J* = 7.6 Hz, 2H), 3.84 (s, 3H), 7.02 (dd, J = 8.8 and 2.4 Hz, 1H), 7.32 (d, *J* = 8.2 Hz, 2H), 7.48 (d, *J* = 8.2 Hz, 2H), 7.55 (s, 1H), 7.63 (d, *J* = 2.4 Hz, 1H), 7.73 (d, *J* = 8.8 Hz, 1H). MS (ESI): $[M + 1]^+$=269.4.

*5.1.2.8. 6-Methoxy-2-(4-methoxyphenyl)benzo[b]thiophene (**7h**).* Following general procedure A, the crude residue purified by flash chromatography, using Et_2O:petroleum ether 0.5:9.5 (v:v) for elution, furnished compound **7 h** as a colorless oil. Yield: 60%. ^{1}H NMR

(DMSO-d_6) δ: 3.82 (s, 3H), 3.84 (s, 3H), 7.02 (dd, J = 9.0 and 2.4 Hz, 1H), 7.06 (d, *J* = 8.8 Hz, 2H), 7.47 (s, 1H), 7.49 (d, *J* = 8.8 Hz, 2H), 7.62 (d, *J* = 2.4 Hz, 1H), 7.70 (d, *J* = 9.0 Hz, 1H). MS (ESI): $[M + 1]^+$=271.1.

*5.1.2.9. 6-Methoxy-2-(3-methoxyphenyl)benzo[b]thiophene (**7i**).* Following general procedure A, the crude residue purified by flash chromatography, using Et_2O:petroleum ether 0.1:9.9 (v:v) for elution, furnished compound **7i** as a colorless oil. Yield: 54%. ^{1}H NMR (DMSO-d_6) δ: 3.83 (s, 3H), 3.84 (s, 3H), 6.97–6.99 (m, 1H), 7.00–7.17 (m, 1H), 7.04 (dd, J = 8.8 and 2.2 Hz, 1H), 7.10–7.17 (m, 1H), 7.42 (t, *J* = 8.0 Hz, 1H), 7.62 (s, 1H), 7.63 (d, *J* = 2.2 Hz, 1H), 7.75 (d, *J* = 9.0 Hz, 1H). MS (ESI): $[M + 1]^+$=271.3.

*5.1.2.10. 2-(4-Ethoxyphenyl)-6-methoxybenzo[b]thiophene (**7j**).* Following general procedure A, the crude residue purified by flash chromatography, using Et_2O:petroleum ether 0.25:9.75 (v:v) for elution, furnished compound **7j** as a white solid. Yield: 54%, mp 82–84 °C. ^{1}H NMR (DMSO-d_6) δ: 1.36 (t, *J* = 7.2 Hz, 3H), 3.84 (s, 3H), 4.07 (q, *J* = 7.2 Hz, 2H), 7.03–7.07 (m, 3H), 7.48 (s, 1H), 7.52 (d, *J* = 8.6 Hz, 2H), 7.62 (d, *J* = 2.2 Hz, 1H), 7.70 (d, *J* = 8.8 Hz, 1H). MS (ESI): $[M + 1]^+$=285.4.

*5.1.2.11. 2-(3-Ethoxyphenyl)-6-methoxybenzo[b]thiophene (**7k**).* Following general procedure A, the crude residue purified by flash chromatography, using Et_2O:petroleum ether 0.1:9.99 (v:v) for elution, furnished compound **7 k** as a clear oil. Yield: 61%. ^{1}H NMR (DMSO-d_6) δ: 1.35 (d, *J* = 7.0 Hz, 3H), 3.84 (s, 3H), 4.08 (q, *J* = 7.0 Hz, 2H), 6.96 (ddd, J = 8.4, 2.6 and 0.8 Hz, 1H), 7.03 (d, *J* = 2.4 Hz, 1H), 7.07–7.09 (m, 1H), 7.11 (dt, J = 7.6 and 1.6 Hz, 1H), 7.41 (t, *J* = 7.6 Hz, 1H), 7.61–7.64 (m, 2H), 7.75 (d, *J* = 9.0 Hz, 1H). MS (ESI): $[M + 1]^+$=285.4.

*5.1.2.12. 6-Methoxy-2-(4-propoxyphenyl)benzo[b]thiophene (**7l**).* Following general procedure A, the crude residue purified by flash chromatography, using Et_2O:petroleum ether 0.5:9.5 (v:v) for elution, furnished compound **7 l** as a clear oil. Yield: 50%. ^{1}H NMR (DMSO-d_6) δ: 1.04 (t, *J* = 7.4 Hz, 3H), 1.72–1.78 (m, 2H), 3.84 (s, 3H), 4.02 (q, *J* = 7.2 Hz, 2H), 7.03–7.08 (m, 3H), 7.48 (s, 1H), 7.49 (d, *J* = 7.6 Hz, 2H), 7.62 (d, *J* = 2.2 Hz, 1H), 7.70 (d, *J* = 8.8 Hz, 1H). MS (ESI): $[M + 1]^+$=299.4.

*5.1.2.13. 2-(4-Butoxyphenyl)-6-methoxybenzo[b]thiophene (**7m**).* Following general procedure A, the crude residue purified by flash chromatography, using Et_2O:petroleum ether 0.25:9.75 (v:v) for elution, furnished compound **7 m** as a clear oil. Yield: 58%. ^{1}H NMR (DMSO-d_6) δ: 0.95 (t, *J* = 7.4 Hz, 3H), 1.44–1.48 (m, 2H), 1.69–1.74 (m, 2H), 3.84 (s, 3H), 4.03 (t, *J* = 6.6 Hz, 2H), 7.02–7.08 (m, 3H), 7.49–7.52 (m, 3H), 7.62 (d, *J* = 2.2 Hz, 1H), 7.70 (d, *J* = 8.8 Hz, 1H). MS (ESI): $[M + 1]^+$=313.4.

*5.1.2.14. 6-Methoxy-2-(4-(pentyloxy)phenyl)benzo[b]thiophene (**7n**).* Following general procedure A, the crude residue purified by flash chromatography, using Et_2O:petroleum ether 0.25:9.75 (v:v) for elution, furnished compound **7n** as a clear oil. Yield: 51%. ^{1}H NMR (DMSO-d_6) δ: 0.88 (t, *J* = 7.2 Hz, 3H), 1.33–1.40 (m, 4H), 1.71–1.74 (m, 2H), 3.80 (s, 3H), 3.99 (t, *J* = 6.4 Hz, 2H), 7.01–7.04 (m, 3H), 7.46–7.49 (m, 3H), 7.60 (d, *J* = 2.4 Hz, 1H), 7.69 (d, *J* = 9.2 Hz, 1H). MS (ESI): $[M + 1]^+$=327.2.

*5.1.2.15. 2-(4-Isopropoxyphenyl)-6-methoxybenzo[b]thiophene (**7o**).* Following general procedure A, the crude residue purified by flash chromatography, using Et_2O:petroleum ether 0.5:9.5 (v:v) for elution, furnished compound **7o** as a white solid. Yield: 57%, mp 93–94 °C. ^{1}H NMR (DMSO-d_6) δ: 1.29 (d, *J* = 5.8 Hz, 6H), 3.84 (s, 3H), 4.63–4.67 (m, 1H), 7.06–7.07 (m, 3H), 7.46–7.51 (m, 3H), 7.61 (d, *J* = 2.2 Hz, 1H), 7.71 (d, *J* = 9.0 Hz, 1H). MS (ESI): $[M + 1]^+$=299.4.

*5.1.3. General procedure b for the preparation of compounds **8a-o** and **9***

To a solution of 6-methoxybenzo[*b*]thiophene **6** or the appropriate 6-methoxy-2-arylbenzo[*b*]thiophene **7a-o** (1 mmol) in THF (5 mL) was added NBS (0.196 g, 1.1 mmol) in small portions at 0 °C. After 1 h at 0 °C, the reaction mixture was allowed to warm to room temperature and stirred for an additional 1 h. The reaction mixture was quenched with 10% aqueous sodium thiosulfate solution at 0 °C (10 mL). The resulting solution was extracted with dichloromethane (3x10 mL), and the combined organic solvent was washed with brine (10 mL), dried and evaporated. The residue was purified by column chromatography on silica gel.

*5.1.3.1. 3-Bromo-6-methoxy-2-phenylbenzo[b]thiophene (**8a**).* Following general procedure B, the crude residue purified by flash chromatography, using Et_2O:petroleum ether 0.25:9.75 (v:v) for elution, furnished compound **8a** as a clear oil. Yield: 67%. ^{1}H NMR (DMSO-d_6) δ: 3.84 (s, 3H), 7.04 (dd, J = 8.8 and 2.4 Hz, 1H), 7.38 (dd, J = 8.6 and 1.8 Hz, 1H), 7.45–7.50 (m, 1H), 7.54–7-60 (m, 1H), 7.61–7.64 (m, 2H), 7.62 (d, *J* = 1.8 Hz, 1H), 7.75 (d, *J* = 9.0 Hz, 1H). MS (ESI): $[M]^+$=318.7, $[M + 2]^+$=320.9.

*5.1.3.2. 3-Bromo-2-(4-fluorophenyl)-6-methoxybenzo[b]thiophene (**8b**).* Following general procedure B, the crude residue purified by flash chromatography, using Et_2O:petroleum ether 0.25:9.75 (v:v) for elution, furnished compound **8b** as a white solid. Yield: 92%, mp 97–98 °C. ^{1}H NMR (DMSO-d_6) δ: 3.82 (s, 3H), 6.99 (dd, J = 8.8 and 2.4 Hz, 1H), 7.32 (s, 1H), 7.34–7.40 (m, 2H), 7.43–7.55 (m, 2H), 7.62 (d, *J* = 2.4 Hz, 1H). MS (ESI): $[M]^+$=337.2, $[M + 2]^+$=339.4.

*5.1.3.3. 3-Bromo-6-methoxy-2-(p-tolyl)benzo[b]thiophene (**8c**).* Following general procedure B, the crude residue purified by flash chromatography, using Et_2O:petroleum ether 0.1:9.9 (v:v) for elution, furnished compound **8c** as a pale yellow oil. Yield: 63%. ^{1}H NMR (DMSO-d_6) δ: 2.38 (s, 3H), 3.84 (s, 3H), 6.92 (dd, J = 8.2 and 2.4 Hz, 1H), 7.34–7.38 (m, 5H), 7.60 (d, *J* = 2.2 Hz, 1H). MS (ESI): $[M]^+$=333.3, $[M + 2]^+$=335.4.

*5.1.3.4. 3-Bromo-6-methoxy-2-(m-tolyl)benzo[b]thiophene (**8d**).* Following general procedure B, the crude residue purified by flash chromatography, using Et_2O:petroleum ether 0.1:9.9 (v:v) for elution, furnished compound **8d** as a colorless oil. Yield: >95%. ^{1}H NMR (DMSO-d_6) δ: 2.40 (s, 3H), 3.82 (s, 3H), 6.98 (dd, J = 9.0 and 2.4 Hz, 1H), 7.23–7.27 (m, 2H), 7.33–7.39 (m, 3H), 7.61 (d, *J* = 2.6 Hz, 1H). MS (ESI): $[M]^+$=333.3, $[M + 2]^+$=335.4.

*5.1.3.5. 3-Bromo-2-(3,4-dimethylphenyl)-6-methoxybenzo[b]thiophene (**8e**).* Following general procedure B, the crude residue purified by flash chromatography, using Et_2O:petroleum ether 2.5:7.5 (v/v) for elution, furnished compound **8e** as a colorless oil. Yield: 89%. ^{1}H NMR (DMSO-d_6) δ: 2.30 (s, 6H), 3.82 (s, 3H), 6.98 (dd, J = 8.8 and 2.4 Hz, 1H), 7.14–7.22 (m, 2H), 7.28–7.37 (m, 2H), 7.59 (d, *J* = 2.2 Hz, 1H). MS (ESI): $[M]^+$=347.3, $[M + 2]^+$=349.4.

*5.1.3.6. 3-Bromo-6-methoxy-2-(3-(trifluoromethyl)phenyl)benzo[b]thiophene (**8f**).* Following general procedure B, the crude residue purified by flash chromatography, using Et_2O:petroleum ether 0.1:9.9 (v:v) for elution, furnished compound **8f** as a colorless oil. Yield: 91%. ^{1}H NMR (DMSO-d_6) δ: 3.83 (s, 3H), 7.00 (dd, J = 9.0 and 2.4 Hz, 1H), 7.53 (d, *J* = 8.8 Hz, 1H), 7.65 (d, *J* = 2.6 Hz, 1H), 7.79–7.82 (m, 3H), 7.86–7.92 (m, 1H). MS (ESI): $[M]^+$=387.3, $[M + 2]^+$=389.4.

*5.1.3.7. 3-Bromo-2-(4-ethylphenyl)-6-methoxybenzo[b]thiophene (**8g**).* Following general procedure B, the crude residue purified by flash chromatography, using Et_2O:petroleum ether 0.25–9.75 (v/v) for elution, furnished compound **8 g** as a pale yellow oil. Yield: 92%. ^{1}H

NMR (DMSO-d_6) δ: 1.26 (t, J = 7.6 Hz, 3H), 2.68 (q, J = 7.6 Hz, 2H), 3.82 (s, 3H), 6.97 (dd, J = 8.8 and 2.4 Hz, 1H), 7.35 (m, 5H), 7.63 (d, J = 2.4 Hz, 1H). MS (ESI): $[M]^+$=347.3, $[M + 2]^+$=349.4.

*5.1.3.8. 3-Bromo-6-methoxy-2-(4-methoxyphenyl)benzo[b]thiophene (**8 h**).* Following general procedure B, the crude residue purified by flash chromatography, using Et_2O:petroleum ether 0.25:9.75 (v:v) for elution, furnished compound **8 h** as a white solid. Yield: 67%, mp 114–116 °C. ^{1}H NMR (DMSO-d_6) δ: 3.80 (s, 3H), 3.83 (s, 3H), 7.00 (dd, J = 9.0 and 2.4 Hz, 1H), 7.04 (d, J = 8.8 Hz, 2H), 7.51 (d, J = 8.8 Hz, 2H), 7.60 (d, J = 2.4 Hz, 1H), 7.72 (d, J = 9.0 Hz, 1H). MS (ESI): $[M]^+$=348.8, $[M + 2]^+$=350.7.

*5.1.3.9. 3-Bromo-6-methoxy-2-(3-methoxyphenyl)benzo[b]thiophene (**8i**).* Following general procedure B, the crude residue purified by flash chromatography, using Et_2O:petroleum ether 0.5:9.5 (v:v) for elution, furnished compound **8i** as a colorless oil. Yield: 94%. ^{1}H NMR (DMSO-d_6) δ: 3.81 (s, 3H), 3.82 (s, 3H), 6.98–7.05 (m, 3H), 7.06–7.19 (m, 1H), 7.37 (d, J = 8.6 Hz, 1H), 7.43 (t, J = 8.6 Hz, 1H), 7.61 (d, J = 2.4 Hz, 1H). MS (ESI): $[M]^+$=349.3, $[M + 2]^+$=351.4.

*5.1.3.10. 3-Bromo-2-(4-ethoxyphenyl)-6-methoxybenzo[b]thiophene (**8j**).* Following general procedure B, the crude residue purified by flash chromatography, using Et_2O:petroleum ether 0.5:9.5 (v:v) for elution, furnished compound **8j** as a white solid. Yield: 95%, mp 91–93 °C. ^{1}H NMR (DMSO-d_6) δ: 1.37 (t, J = 6.8 Hz, 3H), 3.82 (s, 3H), 4.09 (q, J = 6.8 Hz, 2H), 6.97 (dd, J = 9.0 and 2.4 Hz, 1H), 7.06 (J = 9.0 Hz, 2H), 7.48 (s, 1H), 7.34 (dd, J = 8.8 and 2.0 Hz, 2H), 7.59 (d, J = 2.2 Hz, 1H). MS (ESI): $[M]^+$=363.3, $[M + 2]^+$=365.4.

*5.1.3.11. 3-Bromo-2-(3-ethoxyphenyl)-6-methoxybenzo[b]thiophene (**8 k**).* Following general procedure A, the crude residue purified by flash chromatography, using Et_2O:petroleum ether 0.25:9.75 (v:v) for elution, furnished compound **8 k** as a clear oil. Yield: 86%. ^{1}H NMR (DMSO-d_6) δ: 1.35 (d, J = 6.8 Hz, 3H), 3.82 (s, 3H), 4.06 (q, J = 6.8 Hz, 2H), 6.95–6.99 (m, 4H), 7.37–7.43 (m, 2H), 7.61 (d, J = 9.0 Hz, 1H). MS (ESI): $[M]^+$=363.3, $[M + 2]^+$=365.4.

*5.1.3.12. 3-Bromo-6-methoxy-2-(4-propoxyphenyl)benzo[b]thiophene (**8 l**).* Following general procedure B, the crude residue purified by flash chromatography, using Et_2O:petroleum ether 0.25:9.75 (v:v) for elution, furnished compound **8 l** as a clear oil. Yield: 75%. ^{1}H NMR (DMSO-d_6) δ: 1.01 (t, J = 7.4 Hz, 3H), 1.72–1.76 (m, 2H), 3.82 (s, 3H), 3.98 (q, J = 7.2 Hz, 2H), 6.97 (dd, J = 8.8 and 2.4 Hz, 1H), 7.07 (d, J = 8.8 Hz, 2H), 7.35–7.39 (m, 3H), 7.61 (d, J = 2.2 Hz, 1H). MS (ESI): $[M]^+$=377.3, $[M + 2]^+$=379.4.

*5.1.3.13. 3-Bromo-2-(4-butoxyphenyl)-6-methoxybenzo[b]thiophene (**8 m**).* Following general procedure B, the crude residue purified by flash chromatography, using Et_2O:petroleum ether 0.2:9.8 (v:v) for elution, furnished compound **8 m** as a clear oil. Yield: 86%. ^{1}H NMR (DMSO-d_6) δ: 0.96 (t, J = 7.4 Hz, 3H), 1.45–1.49 (m, 2H), 1.67–1.73 (m, 2H), 3.82 (s, 3H), 4.02 (t, J = 6.4 Hz, 2H), 7.02 (dd, J = 8.8 and 2.4 Hz, 1H), 7.07 (d, J = 8.8 Hz, 2H), 7.35–7.39 (m, 3H), 7.59 (d, J = 2.4 Hz, 1H). MS (ESI): $[M]^+$=391.3, $[M + 2]^+$=393.3.

*5.1.3.14. 3-Bromo-6-methoxy-2-(4-(pentyloxy)phenyl)benzo[b]thiophene (**8n**).* Following general procedure B, the crude residue purified by flash chromatography, using Et_2O:petroleum ether 0.25:9.75 (v:v) for elution, furnished compound **8n** as a clear oil. Yield: 85%. ^{1}H NMR (DMSO-d_6) δ: 0.89 (t, J = 7.2 Hz, 3H), 1.34–1.41 (m, 4H), 1.72–1.75 (m, 2H), 3.83 (s, 3H), 3.99 (t, J = 6.4 Hz, 2H), 6.96 (dd, J = 8.8 and 2.4 Hz, 1H), 7.06 (dd, J = 6.4 and 2.0 Hz, 2H), 7.33–7.36 (m, 3H), 7.58 (d, J = 2.0 Hz, 1H), 7.69 (d, J = 9.2 Hz, 1H). MS (ESI): $[M]^+$=405.3, $[M + 2]^+$=407.3.

*5.1.3.15. 3-Bromo-2-(4-isopropoxyphenyl)-6-methoxybenzo[b]thiophene (**8o**).* Following general procedure B, the crude residue purified by flash chromatography, using Et_2O:petroleum ether 0.25:9.75 (v:v) for elution, furnished compound **8o** as a white solid. Yield: 75%, mp 83–85 °C. ^{1}H NMR (DMSO-d_6) δ: 1.32 (d, J = 5.8 Hz, 6H), 3.82 (s, 3H), 4.67–4.72 (m, 1H), 6.97 (dd, J = 8.6 and 2.4 Hz, 1H), 7.05 (d, J = 8.8 Hz, 1H), 7.34–7.38 (m, 3H), 7.59 (d, J = 2.2 Hz, 1H). MS (ESI): $[M]^+$=377.3, $[M + 2]^+$=379.4.

*5.1.3.16. 3-Bromo-6-methoxybenzo[b]thiophene (**9**).* Following general procedure B, the crude residue purified by flash chromatography, using Et_2O:petroleum ether 0.2:9.8 (v:v) for elution, furnished compound **9** as a clear oil. Yield: 65%. ^{1}H NMR (DMSO-d_6) δ: 3.80 (s, 3H), 6.97 (dd, J = 8.8 and 2.4 Hz, 1H), 7.51 (s, 1H), 7.54 (d, J = 2.4 Hz, 1H), 7.66 (d, J = 8.8 Hz, 1H). MS (ESI): $[M]^+$=242.0, $[M + 2]^+$=244.1.

*5.1.4. General procedure C for the preparation of compounds **3a-p***

In a dry glass pressure vessel charged with Ar, a mixture of the appropriate 3-bromo-6-methoxy-2-aryl[*b*]thiophene derivative **8a-o** (1 mmol) or 3-bromo-6-methoxybenzo[*b*]thiophene **9** (243 mg, 1 mmol), 3,4,5-trimethoxyaniline (220 mg, 1.2 mmol, 1.2 equiv.), xanthphos (23 mg, 0.04 mmol, 4 mol%, 30 mg), sodium *tert*-butoxide (0.134 g, 1.40 mmol), and Pd_2dba_3 (18.2 mg, 0.02 mmol, 2 mol%) in dry toluene (5 mL) were added under Ar, and the mixture was heated with stirring at 100 °C for 18 h. After cooling to room temperature, EtOAc was added (5 mL), the mixture was filtered through celite under vacuum and the filtrate diluted with EtOAc (10 mL) and water (5 mL). The aqueous phase was separated and extracted with ethyl acetate (5 mL). The combined organic phases were washed with brine (5 mL), dried over Na_2SO_4 and concentrated under reduced pressure to give a residue, which was purified by chromatography on silica gel.

*5.1.4.1. 6-Methoxy-2-phenyl-N-(3,4,5-trimethoxyphenyl)benzo[b]thiophen-3-amine (**3a**).* Following general procedure C, the crude residue was purified by flash chromatography, using ethyl acetate:petroleum ether 2.5:7.5 (v:v) as eluent, to furnish **3a** as a yellow solid. Yield: 57%, mp 112–114 °C. ^{1}H NMR (DMSO-d_6) δ: 3.55 (s, 3H), 3.62 (s, 6H), 3.81 (s, 3H), 6.17 (s, 2H), 6.94 (dd, J = 8.8 and 2.4 Hz, 1H), 7.22–7.28 (m, 2H), 7.39 (d, J = 8.8 Hz, 1H), 7.47–7.49 (m, 4H), 8.05 (s, 1H). ^{13}C NMR (DMSO-d_6) δ: 55.44 (3C), 60.02, 92.12 (2C), 105.71, 113.91, 122.18, 126.02, 127.11, 128.57 (2C), 129.28 (2C), 130.42, 131.66, 134.07, 135.83, 139.12, 142.26, 153.21 (2C), 156.73. MS (ESI): $[M + 1]^+$=422.0. Anal. calcd for $C_{24}H_{23}NO_4S$: C, 68.39; H, 5.50; N, 3.32; found: C, 68.04; H, 5.26; N, 3.21.

*5.1.4.2. 2-(4-Fluorophenyl)-6-methoxy-N-(3,4,5-trimethoxyphenyl)benzo[b]thiophen-3-amine (**3b**).* Following general procedure C, the crude residue was purified by flash chromatography, using ethyl acetate:petroleum ether 2.5:7.5 (v:v) as eluent, to furnish **3b** as a yellow solid. Yield: 69%, mp 143–145 °C. ^{1}H NMR (DMSO-d_6) δ: 3.53 (s, 3H), 3.62 (s, 6H), 3.79 (s, 3H), 6.15 (s, 2H), 6.93 (dd, J = 8.8 and 2.4 Hz, 1H), 7.26–7.30 (m, 2H), 7.35 (d, J = 9.0 Hz, 1H), 7.37–7.49 (m, 3H), 8.04 (s, 1H). ^{13}C NMR (DMSO-d_6) δ: 55.53 (3C), 60.11, 92.32 (2C), 105.83, 114.02, 115.45, 115.66, 122.09, 124.79, 130.41, 130.62, 131.33, 131.40, 131.67, 135.78, 139.46, 142.17, 153.30 (2C), 156.83, 160.07 and 162.50 ($^1J_{C\text{-}F}$ = 243 Hz). MS (ESI): $[M + 1]^+$=440.4. Anal. calcd for $C_{24}H_{22}FNO_4S$: C, 65.59; H, 5.05; N, 3.19; found: C, 65.38; H, 4.89; N, 3.02.

*5.1.4.3. 6-Methoxy-2-(p-tolyl)-N-(3,4,5-trimethoxyphenyl)benzo[b]thiophen-3-amine (**3c**).* Following general procedure C, the crude residue was purified by flash chromatography, using ethyl acetate:petroleum ether 2.5:7.5 (v:v) as eluent, to furnish **3c** as a yellow solid. Yield: 78%, mp 76–77 °C. ^{1}H NMR (DMSO-d_6)δ: 2.32 (s, 3H), 3.31 (s, 3H), 3.64 (s, 6H), 3.79 (s, 3H), 6.14 (s, 2H), 6.91 (dd, J = 8.8 and 2.4 Hz, 1H), 7.24 (d,

J = 7.6 Hz, 2H), 7.34–7.39 (m, 3H), 7.45 (d, J = 2.4 Hz, 1H), 7.97 (s, 1H). ^{13}C NMR (DMSO-d_6) δ: 21.30, 55.97 (3C), 60.57, 92.54 (2C), 106.24, 114.36, 122.78, 126.70, 129.68 (4C), 130.89, 131.61, 132.27, 136.40, 136.87, 139.23, 142.88, 153.74 (2C), 157.23. MS (ESI): $[M + 1]^+$=436.1. Anal. calcd for $C_{25}H_{25}NO_4S$: C, 68.94; H, 5.79; N, 3.22; found: C, 68.72; H, 5.59; N, 2.98.

*5.1.4.4. 6-Methoxy-2-(m-tolyl)-N-(3,4,5-trimethoxyphenyl)benzo[b]thiophen-3-amine (**3d**).* Following general procedure C, the crude residue was purified by flash chromatography, using ethyl acetate:petroleum ether 2:8 (v:v) as eluent, to furnish **3d** as a yellow solid. Yield: 59%, mp 58–60 °C. ^{1}H NMR (DMSO-d_6) δ: 2.32 (s, 3H), 3.53 (s, 3H), 3.63 (s, 6H), 3.79 (s, 3H), 6.16 (s, 2H), 6.91 (dd, J = 8.8 and 2.4 Hz, 1H), 7.14 (d, J = 7.6 Hz, 1H), 7.22–7.27 (m, 1H), 7.31–7.34 (m, 2H), 7.36 (d, J = 8.8 Hz, 1H), 7.45 (d, J = 2.4 Hz, 1H). 7.99 (s, 1H). ^{13}C NMR (DMSO-d_6) δ: 21.11, 55.51 (3C), 60.10, 92.37 (2C), 105.75, 113.93, 122.27, 125.83, 126.51, 127.84, 128.54, 129.89, 130.55, 131.89, 134.10, 135.74, 137.65, 139.18, 142.25, 153.25 (2C), 156.74. MS (ESI): $[M + 1]^+$=436.4. Anal. calcd for $C_{25}H_{25}NO_4S$: C, 68.94; H, 5.79; N, 3.22; found: C, 68.76; H, 5.61; N, 3.01.

*5.1.4.5. 2-(3,4-Dimethylphenyl)-6-methoxy-N-(3,4,5-trimethoxyphenyl) benzo[b]thiophen-3-amine (**3e**).* Following general procedure C, the crude residue was purified by flash chromatography, using ethyl acetate: petroleum ether 2:8 (v:v) as eluent, to furnish **3e** as a yellow solid. Yield: 74%, mp 73–75 °C. ^{1}H NMR (DMSO-d_6) δ: 2.25 (s, 6H), 3.55 (s, 3H), 3.63 (s, 6H), 3.80 (s, 3H), 6.17 (s, 2H), 6.93 (dd, J = 9.0 and 2.0 Hz, 1H), 7.18–7.24 (m, 2H), 7.25 (s, 1H), 7.37 (d, J = 9.2 Hz, 1H), 7.46 (d, J = 2.2 Hz, 1H), 7.96 (s, 1H). ^{13}C NMR (DMSO-d_6) δ: 19.06, 19.40, 55.41 (3C), 60.02, 92.14 (2C), 105.65, 113.76, 122.26, 126.06, 126.72, 129.64, 130.26 (2C), 131.49, 131.91, 135.08, 135.72, 136.19, 138.64, 142.30, 153.18 (2C), 156.64. MS (ESI): $[M + 1]^+$=450.2. Anal. calcd for $C_{26}H_{27}NO_4S$: C, 69.46; H, 6.05; N, 3.12; found: C, 69.27; H, 5.89; N, 2.97.

*5.1.4.6. 6-Methoxy-2-(3-(trifluoromethyl)phenyl)-N-(3,4,5-trimethoxyphenyl)benzo[b]thiophen-3-amine (**3f**).* Following general procedure C, the crude residue was purified by flash chromatography, using ethyl acetate:petroleum ether 2.5:7.5 (v:v) as eluent, to furnish **3f** as a yellow solid. Yield: 73%, mp 63–64 °C. ^{1}H NMR (DMSO-d_6) δ: 3.54 (s, 3H), 3.63 (s, 6H), 3.81 (s, 3H), 6.18 (s, 2H), 6.96 (dd, J = 8.8 and 2.0 Hz, 1H), 7.36 (d, J = 8.8 Hz, 1H), 7.50 (d, J = 2.0 Hz, 1H), 7.69–7.78 (m, 4H), 8.23 (s, 1H). ^{13}C NMR (DMSO-d_6) δ: 55.42 (3C), 59.99, 92.74 (2C), 105.85, 114.12, 121.48, 122.87, 123.68, 125.62, 129.15, 129.47, 129.72, 130.77, 131.28, 133.37, 135.20, 135.42, 140.81, 141.45, 153.18 (2C), 156.73. MS (ESI): $[M + 1]^+$=490.3. Anal. calcd for $C_{25}H_{22}F_3NO_4S$: C, 61.34; H, 4.53; N, 2.86; found: C, 61.11; H, 4.36; N, 2.72.

*5.1.4.7. 2-(4-Ethylphenyl)-6-methoxy-N-(3,4,5-trimethoxyphenyl)benzo [b]thiophen-3-amine (**3 g**).* Following general procedure C, the crude residue was purified by flash chromatography, using ethyl acetate:petroleum ether 2:8 (v:v) as eluent, to furnish **3 g** as a yellow solid. Yield: 69%, mp 52–54 °C. ^{1}H NMR (DMSO-d_6) δ: 1.21 (t, J = 7.6 Hz, 3H), 2.63 (q, J = 7.6 Hz, 2H), 3.55 (s, 3H), 3.64 (s, 6H), 3.81 (s, 3H), 6.18 (s, 2H), 6.93 (dd, J = 8.8 and 2.4 Hz, 1H), 7.30 (d, J = 8.0 Hz, 2H), 7.39–7.42 (m, 3H), 7.47 (d, J = 2.4 Hz, 1H), 8.01 (s, 1H). ^{13}C NMR (DMSO-d_6) δ: 15.41, 27.86, 55.38, 55.43 (2C), 60.02, 92.07 (2C), 105.69, 113.81, 122.28, 126.17, 127.95 (2C), 129.18 (2C), 130.39, 131.34, 131.74, 135.86, 138.74, 142.39, 142.58, 153.22 (2C), 156.70. MS (ESI): $[M + 1]^+$=450.4. Anal. calcd for $C_{26}H_{27}NO_4S$: C, 69.46; H, 6.05; N, 3.12; found: C, 69.28; H, 5.89; N, 3.01.

*5.1.4.8. 6-Methoxy-2-(4-methoxyphenyl)-N-(3,4,5-trimethoxyphenyl) benzo[b]thiophen-3-amine (**3 h**).* Following general procedure C, the crude residue was purified by flash chromatography, using ethyl acetate: petroleum ether 3:7 (v:v) as eluent, to furnish **3 h** as a light brown solid. Yield: 78%, mp 63–65 °C. ^{1}H NMR (DMSO-d_6) δ: 3.55 (s, 3H), 3.63 (s, 6H), 3.78 (s, 3H), 3.81 (s, 3H), 6.15 (s, 2H), 6.93 (dd, J = 8.8 and 2.4 Hz, 1H), 7.02 (d, J = 6.4 Hz, 2H), 7.39–7.41 (m, 3H), 7.47 (d, J = 2.4 Hz, 1H), 7.96 (s, 1H). ^{13}C NMR (DMSO-d_6) δ: 55.10, 55.52 (3C), 60.12, 92.03 (2C), 105.79, 113.91, 114.12 (2C), 122.40, 126.24, 130.41, 130.52 (2C), 131.95, 135.98, 138.40, 142.54, 153.32 (2C), 156.81, 158.41, 188.31. MS (ESI): $[M + 1]^+$=452.1. Anal. calcd for $C_{25}H_{25}NO_5S$: C, 66.50; H, 5.58; N, 3.10; found: C, 66.36; H, 5.32; N, 2.89.

*5.1.4.9. 6-Methoxy-2-(3-methoxyphenyl)-N-(3,4,5-trimethoxyphenyl) benzo[b]thiophen-3-amine (**3i**).* Following general procedure C, the crude residue was purified by flash chromatography, using ethyl acetate: petroleum ether 2.5:7.5 (v:v) as eluent, to furnish **3i** as a yellow solid. Yield: 71%, mp 58–60 °C. ^{1}H NMR (DMSO-d_6) δ: 3.55 (s, 3H), 3.64 (s, 6H), 3.73 (s, 3H), 3.81 (s, 3H), 6.17 (s, 2H), 6.94 (t, J = 7.6 Hz, 1H), 6.98–7.05 (m, 2H), 7.01–7.06 (m, 1H), 7.36–7.38 (m, 1H), 7.43 (d, J = 8.6 Hz, 1H), 7.48 (d, J = 1.6 Hz, 1H), 8.04 (s, 1H). ^{13}C NMR (DMSO-d_6) δ: 54.87, 55.39, 55.44 (2C), 60.02, 92.19 (2C), 105.68, 112.59, 113.89, 114.89, 121.52, 122.27, 125.74, 129.57, 130.44, 131.64, 135.32, 135.75, 139.20, 142.27, 153.20 (2C), 156.70, 159.26. MS (ESI): $[M + 1]^+$=452.1. Anal. calcd for $C_{25}H_{25}NO_5S$: C, 66.50; H, 5.58; N, 3.10; found: C, 66.40; H, 5.34; N, 2.93.

*5.1.4.10. 6-Methoxy-2-(4-ethoxyphenyl)-N-(3,4,5-trimethoxyphenyl) benzo[b]thiophen-3-amine (**3j**).* Following general procedure C, the crude residue was purified by flash chromatography, using ethyl acetate: petroleum ether 2.5:7.5 (v:v) as eluent, to furnish **3j** as a light brown solid. Yield: 67%, mp 158–160 °C. ^{1}H NMR (DMSO-d_6) δ: 1.34 (t, J = 6.8 Hz, 3H), 3.54 (s, 3H), 3.63 (s, 6H), 3.81 (s, 3H), 4.04 (q, J = 6.8 Hz, 2H), 6.15 (s, 2H), 6.93 (dd, J = 8.8 and 2.4 Hz, 1H), 7.00 (d, J = 8.8 Hz, 2H), 7.37–7.41 (m, 3H), 7.47 (d, J = 2.4 Hz, 1H), 7.96 (s, 1H). ^{13}C NMR (DMSO-d_6) δ: 14.61, 55.42 (3C), 60.02, 62.90, 91.93 (2C), 105.68, 109.63, 113.81, 114.44 (2C), 122.31, 125.99, 126.21, 130.40 (2C), 131.85, 135.88, 138.26, 142.44, 153.20 (2C), 156.71, 157.59. MS (ESI): $[M + 1]^+$=466.0. Anal. calcd for $C_{26}H_{27}NO_5S$: C, 67.08; H, 5.85; N, 3.01; found: C, 66.89; H, 5.69; N, 2.89.

*5.1.4.11. 6-Methoxy-2-(3-ethoxyphenyl)-N-(3,4,5-trimethoxyphenyl) benzo[b]thiophen-3-amine (**3 k**).* Following general procedure C, the crude residue was purified by flash chromatography, using ethyl acetate: petroleum ether 2.5:7.5 (v:v) as eluent, to furnish **3 k** as a yellow solid. Yield: 64%, mp 129–131 °C. ^{1}H NMR (DMSO-d_6) δ: 1.29 (d, J = 6.8 Hz, 3H), 3.55 (s, 3H), 3.64 (s, 6H), 3.81 (s, 3H), 3.98 (q, J = 6.8 Hz, 2H), 6.18 (s, 2H), 6.84–7.01 (m, 4H), 7.34 (t, J = 6.8 Hz, 1H), 7.43–7.47 (m, 4H), 8.03 (s, 1H). ^{13}C NMR (DMSO-d_6) δ: 14.52, 55.39, 55.45 (2C), 60.03, 62.82, 92.21 (2C), 105.68, 113.15, 113.89, 115.25, 121.39, 122.29, 125.83, 129.56, 130.45, 131.66, 135.30, 139.16, 141.25, 142.29, 153.22 (2C), 156.71, 158.54. MS (ESI): $[M + 1]^+$=466.4. Anal. calcd for $C_{26}H_{29}NO_5S$: C, 67.08; H, 5.85; N, 3.01; found: C, 66.85; H, 5.72; N, 2.89.

*5.1.4.12. 6-Methoxy-2-(4-propoxyphenyl)-N-(3,4,5-trimethoxyphenyl) benzo[b]thiophen-3-amine (**3 l**).* Following general procedure C, the crude residue was purified by flash chromatography, using ethyl acetate: petroleum ether 2.5:7.5 (v:v) as eluent, to furnish **3 l** as a yellow solid. Yield: 66%, mp 71–73 °C. ^{1}H NMR (DMSO-d_6) δ: 0.98 (t, J = 7.2 Hz, 3H), 1.74–1.80 (m, 2H), 3.55 (s, 3H), 3.63 (s, 6H), 3.81 (s, 3H), 3.95 (q, J = 7.2 Hz, 2H), 6.15 (s, 2H), 6.94 (dd, J = 8.4 and 2.4 Hz, 1H), 7.01 (d, J = 8.4 Hz, 2H), 7.37–7.41 (m, 3H), 7.47 (d, J = 2.4 Hz, 1H), 7.96 (s, 1H). ^{13}C NMR (DMSO-d_6) δ: 10.89, 22.50, 55.96 (3C), 60.56, 69.35, 92.49 (2C), 106.23, 114.34, 115.03 (2C), 122.84, 126.53, 126.71, 130.94 (2C), 132.40, 136.41, 138.81, 142.97, 141.25, 153.74 (2C), 157.24, 158.28. MS (ESI): $[M + 1]^+$=480.1. Anal. calcd for $C_{27}H_{29}NO_5S$: C, 67.62; H, 6.09; N, 2.92; found: C, 67.45; H, 5.82; N, 2.77.

*5.1.4.13. 2-(4-Butoxyphenyl)-6-methoxy-N-(3,4,5-trimethoxyphenyl) benzo[b]thiophen-3-amine (**3 m**).* Following general procedure C, the crude residue was purified by flash chromatography, using ethyl acetate: petroleum ether 2.5:7.5 (v:v) as eluent, to furnish **3 m** as a yellow solid. Yield: 56%, mp 41–42 °C. ^{1}H NMR (DMSO-d_6) δ: 0.90 (t, J = 7.4 Hz, 3H), 1.41–1.44 (m, 2H), 1.67–1.70 (m, 2H), 3.52 (s, 3H), 3.61 (s, 6H), 3.79 (s, 3H), 3.96 (t, J = 6.4 Hz, 2H), 6.13 (s, 2H), 6.91 (dd, J = 8.8 and 2.4 Hz, 1H), 6.98 (d, J = 8.8 Hz, 2H), 7.35–7.39 (m, 3H), 7.44 (d, J = 2.4 Hz, 1H), 7.94 (s, 1H). ^{13}C NMR (DMSO-d_6) δ: 13.69, 18.76, 30.76, 55.51 (3C), 60.10, 67.09, 92.03 (2C), 105.77, 113.88, 114.56 (2C), 122.39, 126.07, 126.26, 130.48 (3C), 131.93, 135.96, 138.35, 142.51, 153.29 (2C), 156.79, 157.84. MS (ESI): $[M + 1]^+$=494.1. Anal. calcd for $C_{28}H_{31}O_5S$: C, 68.13; H, 6.33; N, 2.84; found: C, 68.01; H, 6.21; N, 2.58.

*5.1.4.14. 6-Methoxy-2-(4-(pentyloxy)phenyl)-N-(3,4,5-trimethoxyphenyl)benzo[b]thiophen-3-amine (**3n**).* Following general procedure C, the crude residue was purified by flash chromatography, using ethyl acetate:petroleum ether 2:8 (v:v) as eluent, to furnish **3n** as a light brown solid. Yield: 56%, mp 117–119 °C. ^{1}H NMR (DMSO-d_6) δ: 0.86 (t, J = 7.2 Hz, 3H), 1.33–1.37 (m, 4H), 1.70–1.74 (m, 2H), 3.52 (s, 3H), 3.61 (s, 6H), 3.79 (s, 3H), 3.95 (t, J = 6.4 Hz, 2H), 6.13 (s, 2H), 6.91 (dd, J = 8.8 and 2.4 Hz, 1H), 6.98 (d, J = 8.8 Hz, 2H), 7.35–7.39 (m, 3H), 7.45 (d, J = 2.4 Hz, 1H), 7.94 (s, 1H). ^{13}C NMR (DMSO-d_6) δ: 13.94, 21.89, 27.74, 28.40, 55.51 (3C), 60.11, 67.39, 92.03 (2C), 105.77, 113.89, 114.56 (2C), 122.39, 126.08, 126.26, 130.48 (2C), 131.94, 135.96, 138.35, 142.51, 153.29 (2C), 156.79, 156.80, 157.84. MS (ESI): $[M + 1]^+$=508.2. Anal. calcd for $C_{29}H_{33}NO_5S$: C, 68.61; H, 6.55; N, 2.76; found: C, 68.46; H, 6.35; N, 2.58.

*5.1.4.15. 2-(4-Isopropoxyphenyl)-6-methoxy-N-(3,4,5-trimethoxyphenyl) benzo[b]thiophen-3-amine (**3o**).* Following general procedure C, the crude residue was purified by flash chromatography, using ethyl acetate: petroleum ether 2.5:7.5 (v:v) as eluent, to furnish **3o** as a yellow solid. Yield: 73%, mp 64–65 °C. ^{1}H NMR (DMSO-d_6) δ: 1.27 (d, J = 6.0 Hz, 6H), 3.55 (s, 3H), 3.63 (s, 6H), 3.81 (s, 3H), 4.62–4.65 (m, 1H), 6.16 (s, 2H), 6.93 (dd, J = 8.8 and 2.4 Hz, 1H), 6.98 (d, J = 8.8 Hz, 2H), 7.36–7.42 (m, 3H), 7.46 (d, J = 2.4 Hz, 1H), 7.97 (s, 1H). ^{13}C NMR (DMSO-d_6) δ: 21.79 (2C), 55.37, 55.42 (2C), 60.01, 68.94, 91.99 (2C), 105.62, 113.78, 115.44 (2C), 122.31, 125.82, 126.05, 130.42 (3C), 131.84, 135.85, 138.26, 142.42, 153.19 (2C), 156.51, 156.68. MS (ESI): $[M + 1]^+$=480.2. Anal. calcd for $C_{27}H_{29}NO_5S$: C, 67.62; H, 6.09; N, 2.92; found: C, 67.39; H, 5.89; N, 2.71.

*5.1.4.16. 6-Methoxy-N-(3,4,5-trimethoxyphenyl)benzo[b]thiophen-3-amine (**3p**).* Following general procedure C, the crude residue was purified by flash chromatography, using ethyl acetate:petroleum ether 3:7 (v:v) as eluent, to furnish **3p** as a red solid. Yield: 62%, mp 68–70 °C. ^{1}H NMR (DMSO-d_6) δ: 3.54 (s, 3H), 3.80 (s, 6H), 3.82 (s, 3H), 6.20 (s, 2H), 6.98 (dd, J = 8.8 and 2.4 Hz, 1H), 7.51 (s, 1H), 7.54 (d, J = 2.4 Hz, 1H), 7.66 (d, J = 8.8 Hz, 1H), 8.75 (s, 1H). ^{13}C NMR (DMSO-d_6) δ: 51.83, 55.88 (3C), 94.36 (2C), 114.76, 118.91, 123.76, 125.22, 126.93, 128.46, 131.20, 134.43, 140.25, 153.52 (2C), 162.57. MS (ESI): $[M + 1]^+$=346.1. Anal. calcd for $C_{18}H_{19}NO_4S$: C, 62.59; H, 5.54; N, 4.06; found: C, 62.45; H, 5.38; N, 3.87.

5.2. Biological assays and computational studies

5.2.1. Initial antiproliferative assays

Human cervix carcinoma (HeLa) and human colorectal adenocarcinoma (HT-29) cells were grown in DMEM medium (Gibco, Milano, Italy). This medium was supplemented with 115 units/mL of penicillin G (Gibco, Milano, Italy), 115 μg/mL streptomycin (Invitrogen, Milano, Italy) and 10% fetal bovine serum (Invitrogen, Milano, Italy). Individual wells of a 96-well tissue culture microtiter plate were inoculated with 100 μL of complete medium containing 8x10^3 cells. The plates were incubated at 37 °C in a humidified 5% CO_2 incubator for 18 h prior to the experiments. After medium removal, 100 μL of the drug solution, dissolved in complete medium at different concentrations, was added to each well and incubated at 37 °C for 72 h. Cell viability was assayed by the (3-(4,5-dimethylthiazol-2-yl)-2,5-diphenyl tetrazolium bromide (MTT) test as previously described [27]. The IC_{50} was defined as the compound concentration required to inhibit cell proliferation by 50%.

5.2.2. Effects on tubulin polymerization and colchicine binding to tubulin

Bovine brain tubulin was purified as described previously [40]. To evaluate the effects of the compounds on tubulin assembly *in vitro* [41], varying concentrations were preincubated with 10 □M tubulin in 0.8 M monosodium glutamate (pH 6.6 with HCl in 2 M stock solution) at 30 ℃ and then cooled to 0 ℃. After addition of GTP, the mixtures were transferred to 0 °C cuvettes in a recording spectrophotometer and warmed to 30 °C, and the assembly of tubulin was observed turbidimetrically. The IC_{50} value was defined as the compound concentration that inhibited the extent of assembly by 50% after a 20 min incubation. Inhibition of colchicine binding to tubulin was measured as described before [42,43], except that the reaction mixtures contained 0.5 μM tubulin, 5 μM [^{3}H]colchicine and 5 μM test compound. Only one DEAE-cellulose filter was used per sample, and filtration was by gravity.

5.2.3. Molecular modeling.

All molecular docking studies were performed on a Viglen Genie Intel®CoreTM i7-3770 vPro CPU@ 3.40 GHz × 8 running Ubuntu 18.04. Molecular Operating Environment (MOE) 2019.10 [44] and Maestro (Schrödinger Release 2020–3) [45] were used as molecular modeling software. The tubulin structure was downloaded from the PDB data bank (http://www.rcsb.org/; PDB code 4O2B). The protein was pre-processed using the Schrödinger Protein Preparation Wizard by assigning bond orders, adding hydrogens and performing a restrained energy minimization of the added hydrogens using the OPLS_2005 force field. Ligand structures were built with MOE and then prepared using the Maestro LigPrep tool by energy minimizing the structures (OPLS_2005 force field), generating possible ionization states at pH 7 ± 2, and generating tautomers and low-energy ring conformers. After isolating a tubulin dimer structure, a 12 Å docking grid (inner-box 10 Å and outer-box 22 Å) was prepared using as centroid the co-crystallized colchicine. Molecular docking studies were performed using Glide SP precision keeping the default parameters and setting 5 as the number of output poses per input ligand to include in the solution. The output database was saved as a mol2 file. The docking results were visually inspected for the quality of binding to the active site.

*5.2.4. Cell death and mitochondrial parameters following **3a** and **3b** treatments*

In all experimental assays, 841 CoN, Caco2 and HCT-116 cells were plated onto 35-mm-well plates and treated for 48 h with vehicle (DMSO), 60 nM **3a** or 400 nM **3b**. Where transfection was required, it was performed before treatment with compounds.

5.2.5. Immunoblot assay

For immunoblotting, cells were lysed in RIPA buffer, protein was quantified by the Lowry method, and 10 μg of protein was loaded into each slot of a 4–20% precast gel. After electrophoretic separation, proteins were transferred onto nitrocellulose membranes that were incubated overnight with the following primary antibodies: actin (as loading marker), cleaved RIP, cleaved caspase 3 and cleaved PARP (for cell death), cyclins A, F, B1 and D1, p27, pHH3 (for cell cycle), MFN1/2 and OPA1 (for mitochondrial dynamics). Protein expression was assessed by specific HRP-labeled secondary antibodies, followed by detection by chemiluminescence using a ChemiDoc™ Touch Gel Imaging System.

5.2.6. Annexin-V assay

Cells were gently harvested, processed with buffers, and incubated

with annexin V-Cy3 solution according to the manufacturer's protocol (Biovision, Milpitas, CA, USA). The green fluorescence signal was quantified under all conditions on a Tali image-based cytometer (Invitrogen).

5.2.7. TALI cell cycle kit

Cells were harvested and centrifuged at 500 × g for 5 min. The medium was discarded and the cells gently resuspended in DPBS, centrifuged at 500 × g for 5 min and transferred to ice. Cells were fixed overnight with ice-cold 70% ethanol in distilled water. The next day, cells were washed, centrifuged and stained with the Tali® Cell Cycle Solution for 30 min. Finally, data were acquired with the Tali® Image-Based Cytometer according to the manufacturer's protocol.

5.2.8. Confocal microscopy analysis

Mitochondrial morphology was assessed after transfecting cells with 2 μg of mtDSred (excitation/emission: 556/586 nm). The mitochondrial membrane potential was assessed by incubating the cells with 10 nM TMRM (excitation/emission: 548/573 nm) for 20 min at 37 °C. Steady-state and poststimulation (FCCP 10 nM) dye intensities were quantified. All the experiments were evaluated with a confocal Nikon Eclipse T_i system. Fluorescent images were captured and analyzed using NisElements 3.2 for membrane potential and Imaris 4.0 software for morphology.

5.2.9. Mitochondrial calcium uptake

Cells were transfected with 2 μg of mtAEQ, the coverslips were incubated with 5 μM coelenterazine for 1.5 h in Krebs-Ringer modified buffer (125 mM NaCl, 5 mM KCl, 1 mM Na_3PO_4, 1 mM $MgSO_4$, 5.5 mM glucose and 20 mM 4-(2-hydroxyethyl)-1-piperazineethanesulfonic acid [HEPES], pH 7.4, at 37 °C) supplemented with 1 mM $CaCl_2$. The agonist (ATP at 100 μM) was added to the same medium. The experiments were terminated by lysing the cells with Triton X-100 in a hypotonic Ca^{2+}-rich solution (10 mM $CaCl_2$ in H_2O), thus discharging the remaining aequorin pool. The light signals were collected and calibrated with [Ca^{2+}] values.

Disclaimer

The authors declare no conflict of interest. This research was supported in part by the Developmental Therapeutics Program in the Division of Cancer Treatment and Diagnosis of the National Cancer Institute, which includes federal funds under Contract No. HHSN261200800001E. The content of this publication does not necessarily reflect the views or policies of the Department of Health and Human Services, nor does mention of trade names, commercial products or organizations imply endorsement by the U.S. Government.

Declaration of Competing Interest

The authors declare that they have no known competing financial interests or personal relationships that could have appeared to influence the work reported in this paper.

Acknowledgment

The authors would like to thank Dr. Alberto Casolari for excellent technical assistance. SF is supported by the Sêr Cymru Programme, which is partially funded by the European Regional Development Fund through the Welsh Government.

Appendix A. Supplementary data

Supplementary data to this article can be found online at https://doi.org/10.1016/j.bioorg.2021.104919.

References

[1] R.S. Wong, Apoptosis in cancer: from pathogenesis to treatment, J. Exp. Clin. Cancer Res. 30 (2011) 87.
[2] L. Ouyang, Z. Shi, S. Zhao, F.T. Wang, T.T. Zhou, B. Liu, J.K. Bao, Programmed cell death pathways in cancer: a review of apoptosis, autophagy and programmed necrosis, Cell Prolif. 45 (2012) 487–498.
[3] R.W. Johnstone, A.A. Ruefli, S.W. Lowe, Apoptosis: a link between cancer genetics and chemotherapy, Cell 108 (2002) 153–164.
[4] F. Mollinedo, C. Gajate, Microtubules, microtubule-interfering agents and apoptosis, Apoptosis 8 (2003) 413.
[5] L. Cirillo, M. Gotta, P. Meraldi, The elephant in the room: the role of microtubules in cancer, Adv. Exp. Med. Biol. 1002 (2017) 93–124.
[6] K.N. Bhalla, Microtubule-targeted anticancer agents and apoptosis, Oncogene 22 (2003) 9075–9086.
[7] M.A. Estève, M. Carré, D. Braguer, Microtubules in apoptosis induction: are they necessary? Curr. Cancer Drug Targets 8 (2007) 713–729.
[8] A. Muroyama, T. Lechler, Microtubule organization, dynamics and functions in differentiated cells, Development 144 (2017) 3012–3021.
[9] C. Garcin, A. Straube, Microtubules in cell migration, Essays Biochem. 63 (5) (2019) 509–520.
[10] C. Janke, The tubulin code: molecular components, readout mechanisms, and functions, J. Cell Biol. 206 (2014) 461–472.
[11] W. Li, H. Sun, S. Xu, Z. Zhu, J. Xu, Tubulin inhibitors targeting the colchicine binding site: a perspective of privileged structures, Future Med. Chem. 9 (2017) 1765–1794.
[12] D. Bates, A. Eastman, Microtubule destabilising agents: far more than just antimitotic anticancer drugs, Br. J. Clin. Pharmacol. 83 (2017) 255–268.
[13] M. Dong, F. Liu, H. Zhou, S. Zhai, B. Yan, Novel natural product- and privileged scaffold-based tubulin inhibitors targeting the colchicine binding site, Molecules 21 (2016) 1375–1400.
[14] R. Kaur, G. Kaur, R.K. Gill, R. Soni, J. Bariwal, Recent developments in tubulin polymerization inhibitors: an overview, Eur. J. Med. Chem. 87 (2014) 89–124.
[15] A.D. Tangutur, D. Kumar, K.V. Krishna, S. Kantevari, Microtubule targeting agents as cancer chemotherapeutics: an overview of molecular hybrids as stabilizing and destabilizing agents, Curr. Top. Med. Chem. 17 (2017) 2523–2537.
[16] Y.N. Cao, L.L. Zheng, D. Wang, X.X. Liang, F. Gao, X.L. Zhou, Recent advances in microtubule-stabilizing agents, Eur. J. Med. Chem. 143 (2018) 806–828.
[17] B. Bhattacharyya, D. Panda, S. Gupta, M. Banerjee, Anti-mitotic activity of colchicine and the structural basis for its interaction with tubulin, Med. Res. Rev. 28 (2008) 155–183.
[18] R.A. Stanton, K.M. Gernert, J.H. Nettles, R. Aneja, Drugs that target dynamic microtubules: a new molecular perspective, Med. Res. Rev. 31 (2011) 443–481.
[19] G.R. Pettit, S.B. Singh, E. Hamel, C.M. Lin, D.S. Alberts, D. Garcia-Kendall, Isolation and structure of the strong cell growth and tubulin inhibitor combretastatin A-4, Experentia 45 (1989) 209–211.
[20] C.M. Lin, H.H. Ho, G.R. Pettit, E. Hamel, Antimitotic natural products combretastatin A-4 and combretastatin A-2: studies on the mechanism of their inhibition of the binding of colchicine to tubulin, Biochemistry 28 (1989) 6984–6991.
[21] E.C. McLoughlin, N.M. O'Boyle, Colchicine-binding site inhibitors from chemistry to clinic: a review, Pharmaceuticals 13 (2020) 8.
[22] L. Li, S. Jiang, X. Li, Y. Liu, J. Su, J. Chen, Recent advances in trimethoxyphenyl (TMP) based tubulin inhibitors targeting the colchicine binding site, Eur. J. Med. Chem. 151 (2018) 482–494.
[23] S. Florian, T.J. Mitchison, Anti-microtubule drugs. Methods, Mol. Biol. 1413 (2016) 403–421.
[24] K.G. Pinney, A.D. Bounds, K.M. Dingerman, V.P. Mocharla, G.R. Pettit, R. Bai, E. Hamel, A new anti-tubulin agent containing the benzo[*b*]thiophene ring system, Bioorg. Med. Chem. Lett. 9 (1999) 1081–1086.
[25] Z. Chen, V.P. Mocharla, J.M. Farmer, G.R. Pettit, E. Hamel, K.G. Pinney, Preparation of new anti-tubulin ligands through a dual-mode, addition-elimination reaction to a bromo-substituted α, β-unsaturated sulfoxide, J. Org. Chem. 65 (2000) 8811–8815.
[26] B.L. Flynn, P. Verdier-Pinard, E. Hamel, A novel palladium-mediated coupling approach to 2,3-disubstituted benzo[*b*]thiophenes and its application to the synthesis of tubulin binding agents, Org. Lett. 3 (2001) 651–654.
[27] R. Romagnoli, P.G. Baraldi, M. Kimatrai Salvador, D. Preti, M. Aghazadeh Tabrizi, M. Bassetto, A. Brancale, E. Hamel, I. Castagliuolo, R. Bortolozzi, G. Basso, G. Viola, Synthesis and biological evaluation of 2-alkoxycarbonyl-3-anilino benzo [*b*]thiophenes and thieno[2,3-*c*]pyridines as new potent anticancer agents, J. Med. Chem. 56 (2013) 2606–2618.
[28] S.L. Graham, K.L. Shepard, P.S. Anderson, J.J. Baldwin, D.B. Best, M.E. Christy, M. B. Freedman, P. Gautheron, C.N. Habecker, J.M. Hoffman, P.A. Lyle, S. R. Michelson, G.S. Ponticello, C.M. Robb, H. Schwam, A.M. Smith, R.L. Smith, J. M. Sondey, K.M. Strohmaier, M.F. Sugrue, S.L. Varga, Topically active carbonic anhydrase inhibitors. 2. Benzo[*b*]thiophenesulfonamide derivatives with ocular hypotensive activity, J. Med. Chem. 32 (1989) 2548–2554.
[29] Z. Xu, Y. Xu, H. Lu, T. Yang, X. Lin, L. Shao, F. Ren, Efficient and C2-selective arylation of indoles, benzofurans, and benzothiophenes with iodobenzenes in water at room temperature, Tetrahedron 71 (2015) 2616–2621.
[30] F. Bray, J. Ferlay, I. Soerjomataram, R.L. Siegel, L.A. Torre, A. Jemal. Global cancer statistics 2018: GLOBOCAN estimates of incidence and mortality worldwide for 36 cancers in 185 countries. CA Cancer J. Clin. 68 (2018) 394-424.
[31] K.J. Basile, A.E. Aplin, Resistance to chemotherapy: short-term drug tolerance and stem cell-like subpopulations, Adv. Pharmacol. 65 (2012) 315–334.

[32] P. Nowak-Sliwinska, L. Scapozza, A.R. Altaba, Drug repurposing in oncology: compounds, pathways, phenotypes and computational approaches for colorectal cancer, Biochim. Biophys. Acta Rev. Cancer 2019 (1971) 434–454.
[33] G.I. Shapiro, J.W. Harper, Anticancer drug targets: cell cycle and checkpoint control, J. Clin. Invest. 104 (1999) 1645–1653.
[34] C. Giorgi, S. Marchi, P. Pinton, The machineries, regulation and cellular functions of mitochondrial calcium, Nat. Rev. Mol. Cell Biol. 19 (2018) 713–730.
[35] I.C.M. Simoes, G. Morciano, M. Lebiedzinska-Arciszewska, G. Aguiari, P. Pinton, Y. Potes, M.R. Wieckowski, The mystery of mitochondria-ER contact sites in physiology and pathology: a cancer perspective, Biochim. Biophys. Acta Mol. Basis Dis. 1866 (2020), 165834.
[36] G. Morciano, G. Pedriali, L. Sbano, T. Iannitti, C. Giorgi, P. Pinton, Intersection of mitochondrial fission and fusion machinery with apoptotic pathways: role of Mcl-1, Biol. Cell 108 (2016) 279–293.
[37] G. Morciano, C. Giorgi, D. Balestra, S. Marchi, D. Perrone, M. Pinotti, P. Pinton, Mcl-1 involvement in mitochondrial dynamics is associated with apoptotic cell death, Mol. Biol. Cell 27 (2016) 20–34.
[38] C. Giorgi, A. Danese, S. Missiroli, S. Patergnani, P. Pinton, Calcium dynamics as a machine for decoding signals, Trends Cell. Biol. 28 (2018) 258–273.
[39] G. Morciano, S. Marchi, C. Morganti, L. Sbano, M. Bittremieux, M. Kerkhofs, M. Corricelli, A. Danese, A. Karkucinska-Wieckowska, M.R. Wieckowski, G. Bultynck, C. Giorgi, P. Pinton, Role of mitochondria-associated ER membranes in calcium regulation in cancer-specific settings, Neoplasia 20 (2018) 510–523.
[40] E. Hamel, C.M. Lin, Separation of active tubulin and microtubule-associated proteins by ultracentrifugation, and isolation of a component causing the formation of microtubule bundles, Biochemistry 23 (1984) 4173–4184.
[41] E. Hamel, Evaluation of antimitotic agents by quantitative comparisons of their effects on the polymerization of purified tubulin, Cell Biochem. Biophys. 38 (2003) 1–21.
[42] E. Hamel, C.M. Lin, Stabilization of the colchicine binding activity of tubulin by organic acids, Biochim. Biophys. Acta 675 (1981) 226–231.
[43] P. Verdier-Pinard, J.-Y. Lai, H.-D. Yoo, J. Yu, B. Marquez, D.G. Nagle, M. Nambu, J. D. White, J.R. Falck, W.H. Gerwick, B.W. Day, E. Hamel, Structure-activity analysis of the interaction of curacin A, the potent colchicine site antimitotic agent, with tubulin and effects of analogs on the growth of MCF-7 breast cancer cells, Mol. Pharmacol. 53 (1998) 62–67.
[44] Molecular Operating Environment (MOE 2019.10); Chemical Computing Group, Inc.: Montreal, Quebec, Canada; URL http://www.chemcomp.com.
[45] Schrödinger Release 2020-3: Maestro, Schrödinger, LLC, New York, NY, 2020.